

COSTS AND BENEFITS OF A PEARL RIVER DELTA EMISSION CONTROL AREA

XIAOLI MAO, CHEN CHEN, BRYAN COMER, PH.D., DAN RUTHERFORD, PH.D.

JULY 2019



icct
THE INTERNATIONAL COUNCIL
ON CLEAN TRANSPORTATION

www.theicct.org

communications@theicct.org

BEIJING | BERLIN | BRUSSELS | SAN FRANCISCO | WASHINGTON

ACKNOWLEDGMENTS

The authors thank members of the International Association for Catalytic Control of Ship Emissions to Air and Dr. Chuansheng Peng for the critical reviews and thoughtful recommendations, and our colleagues Josh Miller, Jennifer Callahan, and Hongyang Cui for their tremendous support in review and proofreading. We especially thank the Health Effects Institute for its generous support in providing mortality data. We also acknowledge Tsinghua University for providing gridded emissions inventory data for land-based sources in China for 2015 and 2030. This study was funded by Energy Foundation China with support from Bloomberg Philanthropies.

International Council on Clean Transportation
1500 K Street NW Suite 650
Washington DC 20005 USA

communications@theicct.org | www.theicct.org | [@TheICCT](https://twitter.com/TheICCT)

© 2019 International Council on Clean Transportation

EXECUTIVE SUMMARY

An Emission Control Area (ECA) is a special area designated by the International Maritime Organization (IMO)—the specialized United Nations agency responsible for regulating international shipping—where a country or group of countries can enforce more stringent air emission standards to improve air quality and protect the environment. There are currently four ECAs in the world, each protecting densely populated coastal regions that experience heavy ship traffic. Although China has one of the most densely populated coastal areas on Earth and is home to some of the world’s busiest ports, it is not protected by an ECA. Research estimates that about 22,000 Chinese die prematurely each year as a consequence of ship-related air pollution. Put another way, each year, one out of every three premature deaths from ship-related air pollution globally occurs in China. To reduce these negative consequences, China could apply to the IMO for an ECA.

To justify ECA designation, countries must demonstrate that (1) shipping is a significant source of emissions that have negative health impacts, and (2) the cost of reducing emissions from ships is comparable to land-based controls. In this paper, we analyze the costs and benefits of a potential Chinese ECA within the Greater Pearl River Delta (GPRD) region in 2030. We assume that the ECA extends 200 nautical miles (nm) from the coast and that all of its provisions are fully in effect by 2025. We focus on the GPRD region because it is densely populated and home to three of the world’s busiest container ports.

We find that, compared with business as usual (BAU), an ECA could reduce sulfur oxides (SO_x) by more than 70%, particulate matter (PM_{10}) by more than 50%, and nitrogen oxides (NO_x) by 12% in 2030 (see Figure ES-1).

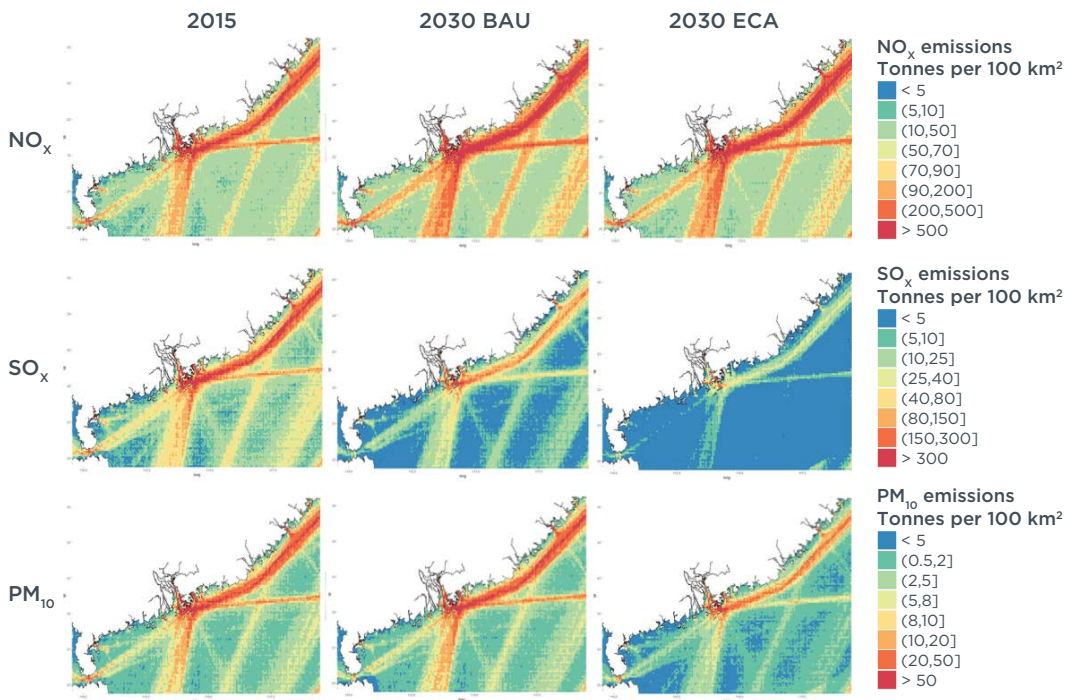


Figure ES-1. Distribution of ship emissions in the GPRD region in 2015 and 2030, BAU versus with an ECA.

Additionally, our results indicate that, across the entire GPRD region, implementing an ECA would reduce ambient fine particulate matter concentrations by 2.3% and ground-level ozone concentrations by 1%, both when compared to a no-ECA scenario in 2030. Although this may seem like a small effect, it translates into substantial health benefits. In 2030, an ECA could avoid about 1,400 premature deaths in the GPRD region, or about one quarter of all shipping deaths that year without an ECA. This would result in economic benefits of about \$1.65 billion (all monetary figures are in 2012 U.S. dollars, unless otherwise indicated) each year.

The estimated cost effectiveness of the ECA in 2030, defined as the cost of compliance per tonne (t) of pollutants abated, is approximately \$4,400 for SO_x, \$16,000 for PM₁₀, and \$680 for NO_x. The cost of complying with the ECA regulations, including the cost of switching to low-sulfur marine fuels and NO_x aftertreatment technologies for new ships, is between \$282 million and \$426 million within the GPRD. The benefit-cost ratio, determined by dividing the monetized health benefits by the costs of compliance, ranges from about 4:1 to 6:1 (see Figure ES-2). The net benefits are in the range of \$1.23 billion to \$1.37 billion. These results demonstrate that a Chinese ECA can be highly cost effective in reducing criteria pollutants like SO_x, PM₁₀, and NO_x.

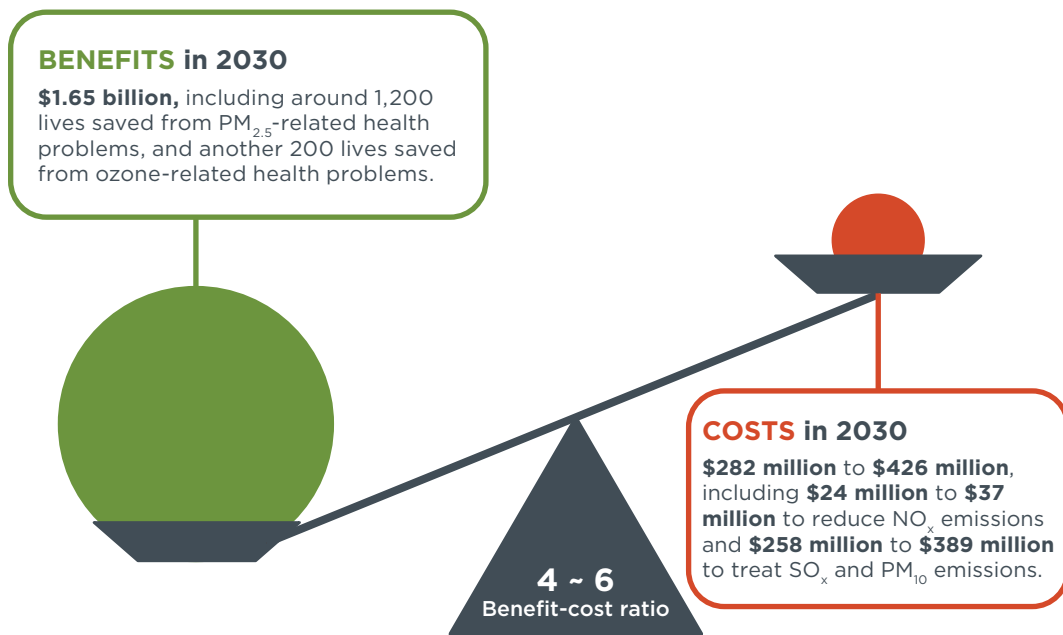


Figure ES-2. Benefit-cost ratio for the GPRD region for a 200-nm Chinese ECA.

TABLE OF CONTENTS

EXECUTIVE SUMMARY	i
LIST OF TABLES	iv
LIST OF FIGURES	v
ABBREVIATIONS	vi
1. INTRODUCTION AND BACKGROUND	1
1.1 SHIPPING IN THE GREATER PEARL RIVER DELTA REGION	1
1.2 AIR POLLUTION AND HEALTH CONSEQUENCES FROM SHIPPING EMISSIONS..	2
1.3 POLICY BACKGROUND	2
2. METHODOLOGY	6
2.1 EMISSIONS.....	6
2.2 AIR-QUALITY MODELING	11
2.3 HEALTH IMPACT ANALYSIS AND VALUATION.....	12
2.4 COST ANALYSIS	14
3. RESULTS AND DISCUSSION	16
3.1 SHIP EMISSIONS	16
3.2 AIR QUALITY	17
3.3 HEALTH BENEFITS	19
3.4 COSTS TO SHIPOWNERS	24
4. CONCLUSIONS	30
REFERENCES	31
APPENDIX: COST SENSITIVITY	36

LIST OF TABLES

Table 1. IMO NO _x emission standards	4
Table 2. Policy adjustment factors for SO _x , PM ₁₀ , and NO _x in emissions projection.....	10
Table 3. Scenarios and main inputs for air quality modeling	11
Table 4. Key inputs and assumptions to run the WRF-Chem model.....	12
Table 5. NO _x control cost functions.....	15
Table 6. Ship emissions within Domain 3, in 2015, 2030 BAU, and 2030 ECA-control scenarios	16
Table 7. Shipping contribution to PM _{2.5} and ozone concentrations and ECA effectiveness in 2030 in GPRD cities.....	18
Table 8. Expected health and economic benefits in 2030 from an ECA in the GPRD region.....	19
Table 9. BAU and ECA-reduced premature mortality associated with acute exposure to ship-related PM _{2.5} in 2030	20
Table 10. BAU and ECA-reduced premature mortality associated with chronic exposure to ship-related PM _{2.5} in 2030.....	20
Table 11. BAU and ECA-reduced premature mortality associated with acute exposure to ship-related ozone in 2030.....	22
Table 12. BAU and ECA-reduced premature mortality associated with chronic exposure to ship-related ozone in 2030.....	22
Table 13. ECA-reduced morbidity in the GPRD region due to reduced PM ₁₀ concentration.	23
Table 14. Cost-effectiveness of fuel-switching for ECA compliance compared to other sulfur control programs	24
Table 15. Cost effectiveness of ECA Tier III NO _x compliance compared to other NO _x control programs.....	25
Table 16. Cost analysis results from the sensitivity analysis.....	25
Table 17. Benefits and costs analysis for the GPRD region from the sensitivity analysis.....	28
Table A1. Fuel price estimates for 2030.....	36
Table A2. Fuel price differential scenarios and cost-effectiveness of fuel-switching	36
Table A3. CAPEX input scenarios and cost-effectiveness of NO _x Tier III compliance	36

LIST OF FIGURES

Figure ES-1. Distribution of ship emissions in the GPRD region in 2015 and 2030, BAU versus with an ECA.	i
Figure ES-2. Benefit-cost ratio for the GPRD region for a 200-nm Chinese ECA.	ii
Figure 1. Oceangoing vessel traffic, port cities, and population in the GPRD region in 2015.	1
Figure 2. Existing Emission Control Areas.	3
Figure 3. IMO marine fuel sulfur regulations inside and outside ECAs.	4
Figure 4. China's domestic emission control areas.	5
Figure 5. Study region (Domain 1), with two additional, nested domains (Domain 2 and Domain 3) defined for air-quality modeling.	8
Figure 6. Distribution of NO _x , SO _x , and PM ₁₀ tailpipe emissions from ships in 2015 and 2030, BAU versus with an ECA.	17
Figure 7. Distribution of avoided PM _{2.5} chronic mortality in 2030 due to ECA controls.	21
Figure 8. Distribution of avoided ozone chronic mortality in 2030 due to ECA controls.	23
Figure 9. Cost analysis boundaries for the GPRD region.	26
Figure 10. Costs and benefits of a 200-nm ECA in the GPRD region.	27
Figure 11. Benefit-cost ratio for the GPRD region for a 200-nm Chinese ECA.	27
Figure 12. Annual discounted costs and benefits of national motor vehicle emission control programs in China, 2015–2045 (Shao & Wagner, 2015).	29

ABBREVIATIONS

AIS	Automatic Identification System
CAPEX	Capital cost
DECA	Domestic Emission Control Areas
ECA	Emission Control Area
EEDI	Energy Efficiency Design Index
EGR	Exhaust gas recirculation
GPRD	Greater Pearl River Delta
IMO	International Maritime Organization
LNG	Liquified natural gas
MADE/ SORGAM	Modal Aerosol Dynamics Model for Europe with the Secondary Organic Aerosol Model
MARPOL	International Convention for the Prevention of Pollution from Ships
MEPC	Marine Environment Protection Committee
OGV	Oceangoing vessel
REAS	Regional Emission Inventory in Asia
RPM	Revolutions per minute
RR	Relative risk
SAVE	Systematic Assessment of Vessel Emissions
SCR	Selective catalytic reduction
SFOC	Specific fuel oil consumption
UNCTAD	United Nations Conference on Trade and Development
VSL	Value of a statistical life
WRF-Chem	Weather Research and Forecasting Model coupled with Chemistry

1. INTRODUCTION AND BACKGROUND

1.1 SHIPPING IN THE GREATER PEARL RIVER DELTA REGION

China's Greater Pearl River Delta (GPRD) region is home to 11 major port cities that together handled approximately 39% of all Chinese outbound trade in 2015. Three of these ports are among the 10 largest container ports in the world: Shenzhen (3), Hong Kong (6), and Guangzhou (7). The ports in the GPRD region together process the largest volume of containerized cargo throughput in the world (Mao, Cui, Roy, Olmer, Rutherford, & Comer, 2017). Oceangoing vessels (OGVs), a major transportation mode for international trade, frequent the GPRD region to load and unload both cargo and passengers. Container ships, bulk carriers, chemical tankers, general cargo vessels, and roll-on/roll-off (ro-ro) ships represented more than 90% of the total gross tonnage (2.7 billion tonnes) of ships visiting this region in 2015 (Mao et al., 2017). Figure 1 shows the high OGV traffic density in this region and its proximity to densely populated areas.

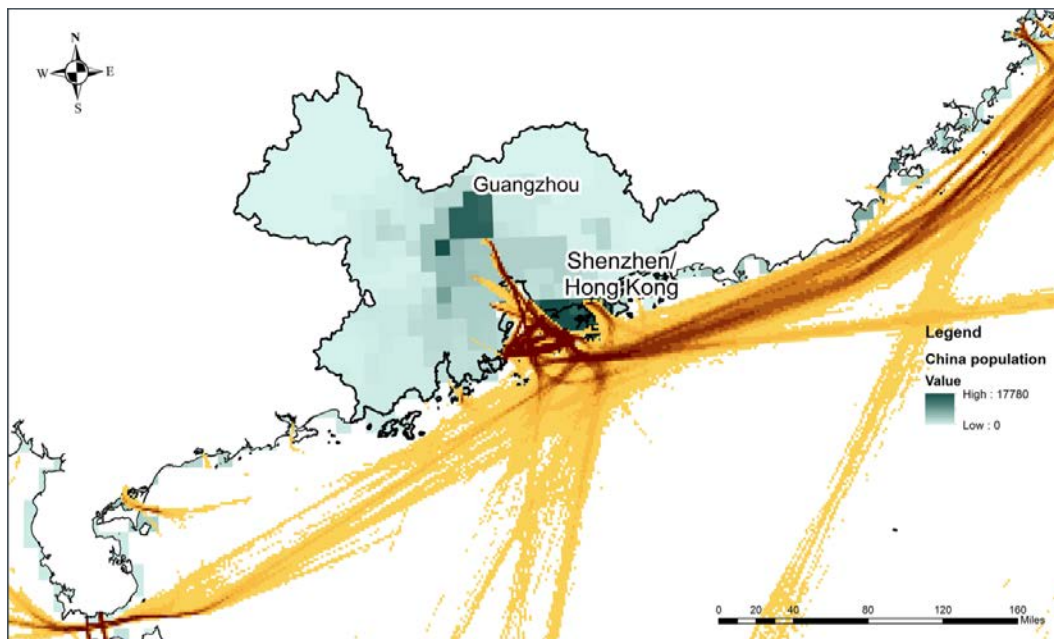


Figure 1. Oceangoing vessel traffic, port cities, and population in the GPRD region in 2015.

Not shown in Figure 1 are non-OGVs, namely Chinese vessels engaged in domestic navigation. Mao and Rutherford (2018b) estimate that within the South China Sea, these ships could emit half as much nitrogen oxides (NO_x) as OGVs. But because many non-OGVs are covered under domestic regulations, and many of these ships do not use equipment to transmit their location and speed, this report focuses only on OGVs.

1.2 AIR POLLUTION AND HEALTH CONSEQUENCES FROM SHIPPING EMISSIONS

Like most other transportation modes, OGVs burn fossil fuels and pollute the air. But unlike other modes, these ships burn the lowest-quality and dirtiest transportation fuels. Until 2020, International Maritime Organization (IMO) rules state that ship fuels can contain up to 35,000 parts per million (ppm) sulfur. After 2020, the maximum allowed sulfur content—the IMO 2020 global sulfur limit—will drop to 5,000 ppm. Within IMO-designated Emission Control Areas (ECAs), however, ships are required to use fuels with no more than 1,000 ppm sulfur or an equivalent compliance mechanism such as a scrubber. In China, Domestic Emission Control Areas (DECAs) cover a portion of the coastline—out to 12 nautical miles (nm)—and require early use of 5,000 ppm fuels. In contrast, the sulfur limit for on-road diesel fuel in China is 10 ppm.

When ships burn fossil fuels, the resultant emissions increase atmospheric concentrations of ambient fine particulate matter (PM_{2.5}) and ground-level ozone. These pollutants harm human health by contributing to respiratory infections, cardiovascular disease, and lung cancer. A recent report estimated that, conservatively, emissions from international shipping caused 60,000 premature deaths globally in 2015 (Anenberg, Miller, Henze, & Minjares, 2019). More than one-third of those deaths, 37%, occurred in China (Rutherford & Miller, 2019). In their log-linear concentration-response results, Sofiev et al. (2018) estimated that shipping-related PM_{2.5} concentrations would cause more than 100,000 deaths per year in 2020 and beyond.

Several recent studies have examined the impact of ship emissions on the air quality of coastal cities in China. Zhang et al. (2017) conducted a high-level review of ship emissions and their atmospheric impacts in China. Chen et al. (2018) and Liu et al. (2018) evaluated the regional air quality impact of shipping in Bohai Rim and the GPRD, respectively. Based on 2015 automatic identification system (AIS) data, Lv et al. (2018) performed the most recent evaluation of ship emissions' impact on PM_{2.5} pollution in China on a national scale. Lin et al. (2018) conducted a time-series study and showed that ship emissions were associated with a more than 5% increase in cardiovascular mortality in Guangzhou.

1.3 POLICY BACKGROUND

1.3.1. Emission Control Areas

Under Annex VI of the International Convention for the Prevention of Pollution from Ships, 1973 as modified by the Protocol of 1978, special areas, called Emission Control Areas (ECAs), can be created. In these areas, higher fuel quality is required and more stringent NO_x emission limits beyond the minimum global standards set by the IMO may apply.

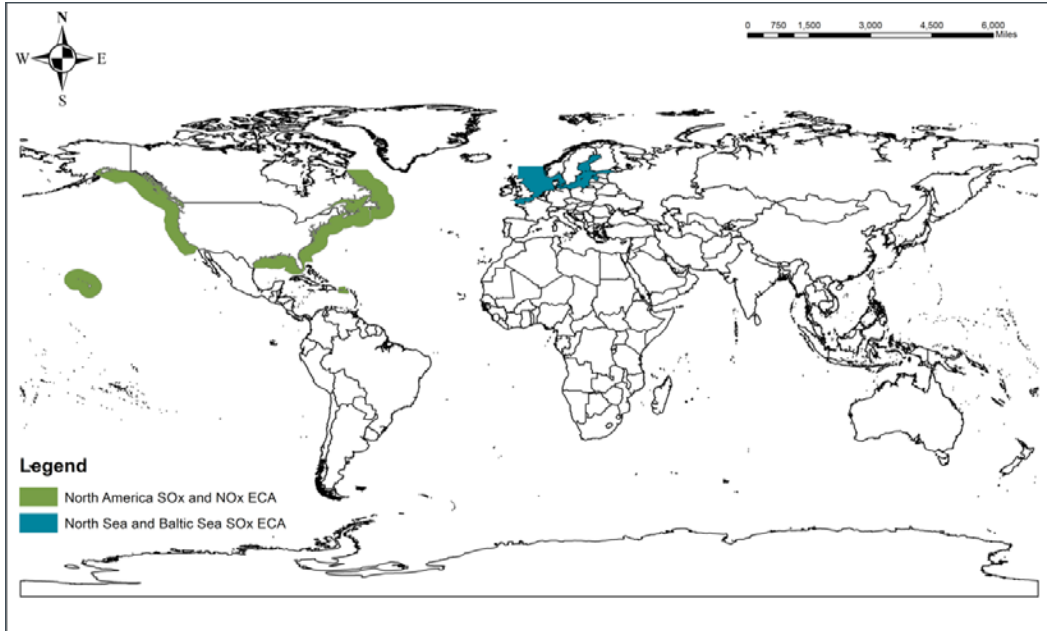


Figure 2. Existing Emission Control Areas.

ECAs are designed to reduce air pollution that can harm human health. Currently, there are four IMO-designated ECAs in the world (Figure 2).¹ In these areas, all ships are required to burn lower-sulfur fuel (see Figure 3 for details) or achieve equivalent compliance using exhaust gas cleaning systems, often called scrubbers. New ships built after a defined date—2016 for the North American and U.S. Caribbean Sea ECAs, and 2021 for the Baltic and North Sea ECAs—are required to achieve more stringent (Tier III) NO_x emissions standards when operating in these ECAs (see Table 1). According to the U.S. Environmental Protection Agency (EPA, 2009), the North American ECA is expected to prevent between 3,800 and 9,500 premature deaths in the United States per year beginning in 2020.

¹ The North America and U.S. Caribbean ECAs control both SO_x and NO_x. The North Sea and Baltic Sea ECAs currently control SO_x only, but they will also control NO_x emissions from new-build ships beginning in 2021.

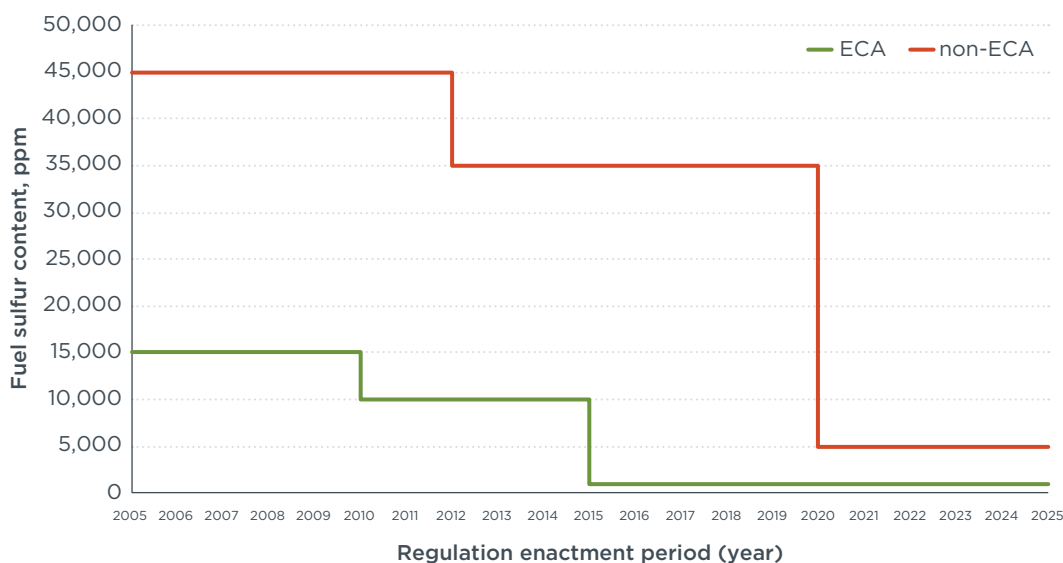


Figure 3. IMO marine fuel sulfur regulations inside and outside ECAs.

Table 1. IMO NO_x emission standards

IMO Tier	Ship construction date on or after	Total weighted cycle emission limit (g/kWh)		
		n ^a < 130	n = 130 - 1999	n ≥ 2,000
I	1 January 2000	17.0	45*n ^{-0.2}	9.8
II	1 January 2011	14.4	44*n ^{-0.23}	7.7
III	1 January 2016 for ships operating in the North American and U.S. Caribbean Sea ECAs	3.4	9*n ^{-0.2}	2.0
	1 January 2021 for ships operating in the Baltic and North Sea ECAs			

^[a] Engine's rated speed (rpm).

1.3.2. China's Domestic Emission Control Areas

Although China has not applied for an IMO-designated ECA, the government has established three regional DECAs since 2016 (Mao, 2016), and one of these covers the GPRD region (see Figure 4). Beginning in 2019, most ships operating within the GPRD regional DECAs are required to operate on marine fuel containing less than 5,000 ppm sulfur.

China's Ministry of Transport recently released an action plan to upgrade the regional DECA system to a national DECA starting January 1, 2019 (Mao, 2019). The national DECA covers the entire coastline within China's territorial sea, out to 12 nm, tightening the fuel sulfur content requirement to 1,000 ppm in two inland waterway systems and also around Hainan Island, and adds progressively tighter NO_x engine controls. In addition, in August 2018, the municipality of Shenzhen began providing financial incentives for ships burning 1,000 ppm or lower sulfur content fuel that visit the Port of Shenzhen.

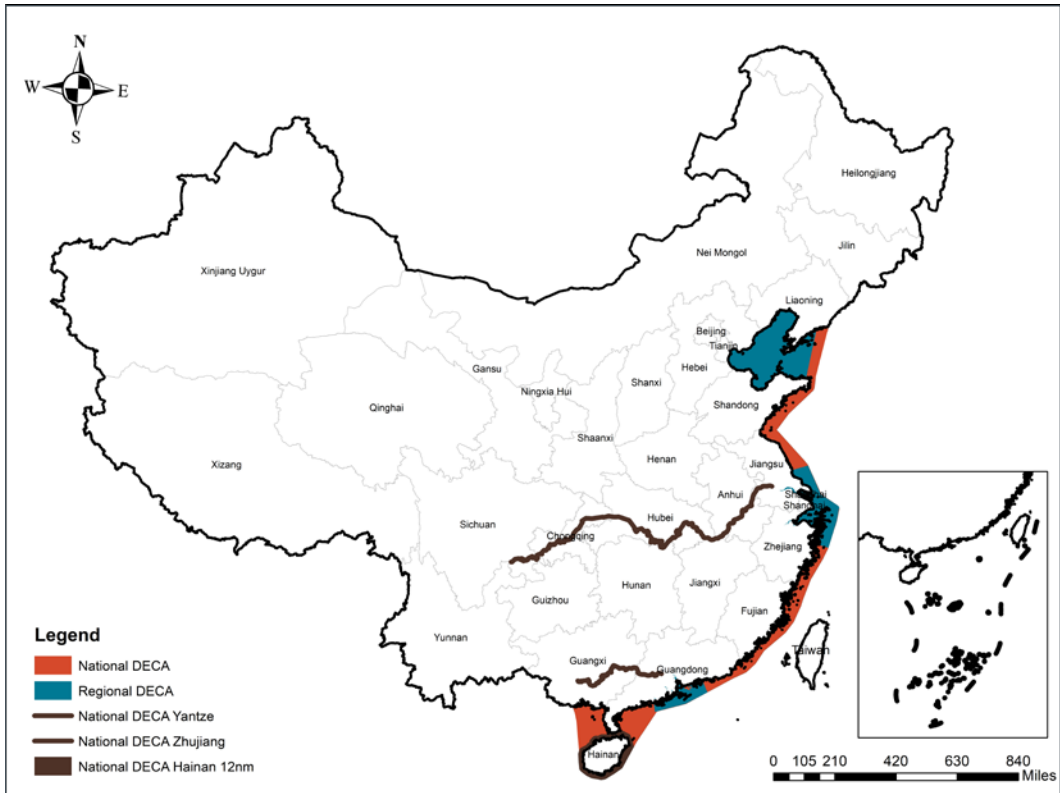


Figure 4. China's domestic emission control areas.

2. METHODOLOGY

This white paper quantifies the $PM_{2.5}$ and ground-level ozone-attributable health impacts in the GPRD region that are associated with ship emissions. It accounts for both the expected contribution of ship emissions to adverse health impacts on land and the reductions in adverse health impacts that are expected from the adoption of the proposed ECA in 2030. A detailed review of our methodology is included in supporting materials to this report. This chapter explains our analytical framework and relates how we calculated emissions and conducted the air-quality modeling.

Our analytical framework is explained the following sections:

- » *Section 2.1* Based on 2015 ship emissions data, we project 2030 ship emissions under two scenarios—a business-as-usual (BAU) scenario and an ECA-control scenario where a 200-nm IMO-designated ECA around China’s coastline takes effect in 2025.
- » *Section 2.2* With the 2030 land-based emissions inventory, we model BAU and ECA-control ambient concentrations of $PM_{2.5}$ and ground-level ozone in 2030. The same air-quality model is used to estimate ambient concentrations of $PM_{2.5}$ and ground-level ozone in 2030 without ship emissions to help determine the baseline impact of ship emissions on air quality.
- » *Section 2.3* The public health impacts of each scenario (BAU scenario and the ECA-control scenario) in 2030 are evaluated. This is done by using the expected change in ambient concentrations and epidemiologically derived health impact functions to model changes in the incidence of health effects that are attributable to shipping.
- » *Section 2.4* The costs of complying with the proposed ECA are assessed. Results are presented in terms of cost per tonne for NO_x , SO_x , and PM abatement and compared with other ECAs. We also calculate the net-benefit and benefit-cost ratio of the ECA policy in the GPRD region.

2.1 EMISSIONS

The 2015 ship emissions inventory was retrieved from our Systematic Assessment of Vessel Emissions (SAVE) model. The underlying data is a global, geospatial dataset of hourly ship activity and associated emissions, which can be aggregated to preferred spatial resolution and output as a gridded emissions inventory. See Olmer, Comer, Roy, Mao, and Rutherford (2017) for the detailed methodology behind the SAVE model.

For this analysis, we geo-fenced the 2015 geospatial ship emissions inventory using coordinates bounded by our study region (see Figure 5). The entire study region is captured in Domain 1 with a 36×36 km horizontal grid spacing. Two nested domains (Domain 2 and Domain 3) have finer resolutions of 12×12 km and 4×4 km, respectively. They were created for the air-quality modeling described in Section 2.2. The 2015 emissions were first projected to 2030 by applying a scaling factor to account for the change in ship traffic expected from growth in trade over this period. Section 2.1.1 describes how these scaling factors were derived. As the fleet will also naturally become more energy efficient over this period, there will be an impact on fuel consumption. Section 2.1.2 introduces the fleet turnover model used to derive the efficiency adjustment factors to adjust the 2030 projection. The policy-related adjustments are then applied and described in Section 2.1.3. Together, this results in the 2030 BAU ship

emissions inventory and the 2030 ECA-control ship emissions inventory. The process can be described by the following equation:

$$E_{i,j,2030} = \sum_{t=0}^{t=n} (E_{i,j,2015} \times TSF_k \times EAF_k \times PAF_{j,l})$$

Where:

- i = ship i
- j = pollutant j
- k = ship class k , which ship i belongs to
- l = ship engine type l , which corresponds to ship i
- $E_{i,j,2030}$ = emissions (g) for ship i and pollutant j in 2030
- $E_{i,j,2015}$ = emissions (g) for ship i and pollutant j in 2015
- TSF_k = trade scale factor for ship class k
- EAF_k = efficiency adjustment factor for ship class k
- $PAF_{j,l}$ = policy adjustment factor for pollutant j and engine type l

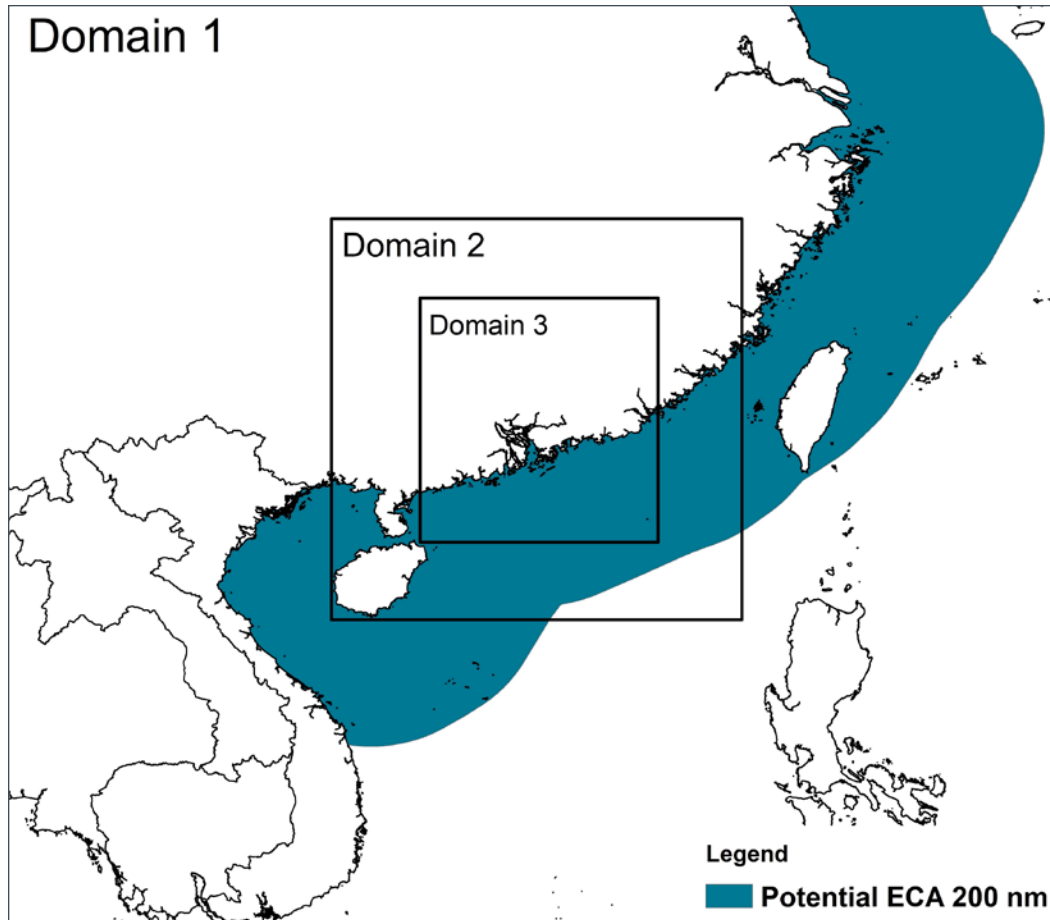


Figure 5. Study region (Domain 1), with two additional, nested domains (Domain 2 and Domain 3) defined for air-quality modeling.

2.1.1. Trade scale factors by ship class due to trade growth

As trade grows, demand for shipping activity grows. Holding everything else constant, growth in trade will proportionally increase fuel consumption and thus air pollution. Trade scale factors are cargo-specific. Each year, the United Nations Conference on Trade and Development (UNCTAD) publishes seaborne trade volumes (in tonnes) by region and by major cargo type. UNCTAD (2017) estimated that from 2017 to 2022, shipping of containerized cargo would grow at an average annual rate of 5% and growth crude oil would be almost flat at an annual rate of 0.9%. To project trade growth out to 2030, we used linear and nonlinear statistical models and UNCTAD data for Asian developing countries from 2006 to 2015. Available data allow us to model the compound growth rates (TSF_k) for four cargo types—containerized cargo, dry bulk, crude oil, and liquified natural gas—over the period of 2016 to 2030.

There have been dedicated studies on trade growth projection and they cover various time spans. Indeed, UNCTAD's *Review of Maritime Transport* (2017) includes a summary of growth projections made by various entities. Our projections here are generally within the range of the cited values. For cargo types for which UNCTAD (2017) does not provide specific historical data, we adopt the average annual growth rate of 2.7% provided by IHS Markit (UNCTAD, 2017). This is because it was made in the time span most relevant for our analysis, 2016–2030. The TSF_k for these cargo types are thus an aggregated growth rate between 2015 and 2030 calculated as such:

$$TSF_k = (1 + ATSF_k)^m$$

Where:

m = number of accumulating years

$ATSF_k$ = annual trade scale factor for ship class k

2.1.2. Efficiency adjustment factors due to fleet turnover

Fuel savings are economically attractive to carriers and newer ships are, unsurprisingly, more energy-efficient than older ones. Our fleet-turnover model is adapted from the one used in the technical support document for the North American ECA application (U.S. Environmental Protection Agency [EPA], 2009), with the following assumptions:

- » The population of the fleet remains unchanged over time
- » A ship's useful life is 25 years
- » Each year, ships that reach the end of their useful life are replaced with new ships built in that year that have average ship characteristics of the existing fleet

Holding cargo transport demand constant, as the fleet turns over, annual fuel consumption and emissions increase with power demand and decrease as cargo-carrying capacity expands. This is because greater power demand means a higher rate of daily fuel consumption and more cargo carried per voyage means fewer voyages and days spent at sea.

In addition to natural turnover, there is the IMO's Energy Efficiency Design Index (EEDI), which requires new-build ships to become more energy efficient over time. For example, ships built after 2025 must be 30% less carbon intensive than a predefined EEDI baseline (Hon & Wang, 2011). Based on a gradually decreasing survival rate for a fleet with increasingly longer in-service history (Wang & Lutsey, 2013), we estimated that implementing current EEDI standards will bring down fuel consumption by about 20% in 2030. To account for EEDI impact on projected emissions in 2030, this study adopts this 20% number to construct the efficiency adjustment factor. Our assumption is similar to the 22.5% used for the *Third IMO Greenhouse Gas Study 2014* (Smith et al., 2015).²

As a result, the efficiency adjustment factors (EAF_k) are calculated with the following equation:

$$EAF_k = \frac{P_{k,2030}}{P_{k,2015}} \times \frac{DWT_{k,2015}}{DWT_{k,2030}} \times (1 - 20\%)$$

Where:

$P_{k,2030}$ = average power demand (kW) for ship class k in 2030

$P_{k,2015}$ = average power demand (kW) for ship class k in 2015

$DWT_{k,2015}$ = average deadweight tonnage, a surrogate for cargo carriage per voyage, for ship class k in 2015

$DWT_{k,2030}$ = average deadweight tonnage, a surrogate for cargo carriage per voyage, for ship class k in 2030

² In May 2019, the IMO accelerated and tightened EEDI energy efficiency targets for some ship types (Comer & Rutherford, 2019). Our modeling was not subsequently updated, but we do not expect the overall findings to be sensitive to this change.

2.1.3 Policy adjustment factors under BAU and ECA-control scenarios

Emission factors, multiplied by fuel consumption, determine the amount of emissions for different pollutants. They vary by ship engine type, fuel type, and, importantly, environmental regulations. ECAs are designed to control conventional air pollutants including SO_x, NO_x, and PM, and thus future emissions of these pollutants within ECAs need to be adjusted accordingly. There is also the need to account for existing global policies that take effect after 2015.

The ECA-related policy adjustment factors ($PAF_{j,l}$) for different pollutants and engine types are derived from the SAVE model (see Olmer et al., 2017 and the supporting materials). The SAVE model used those $PAF_{j,l}$ to adjust emissions within ECAs in 2015. $PAF_{j,l}$ s that relate to Chinese ship control policies taking effect after 2015 other than an ECA are calculated based on the same methodology. NO_x emission factors are more complicated because the IMO regulates NO_x by tiers that relate to when the ship was built (see Table 1) and when the ECA enters into force. Because we assume the Chinese ECA will be in place in 2025, only the NO_x emission factors for ships built after 2025 that need to navigate in this particular ECA are adjusted to reflect Tier III compliance.

Table 2 summarizes $PAF_{j,l}$ values in 2030 under the BAU and ECA-control scenarios. Consistent with the *Third IMO Greenhouse Gas Study* (Smith et al., 2015), we evaluated PM emissions as PM₁₀ because their emission factors are virtually the same for diesel-based fuels.³

Table 2. Policy adjustment factors for SO_x, PM₁₀, and NO_x in emissions projection

Pollutants	Scenarios	Locations	Policy adjustment factors		2030 policies
			2015	2030	
SO _x	ECA-control	Inside ECA	1	0.04	Fuel sulfur content <= 0.1% m/m
		Outside ECA		0.2	Fuel sulfur content <= 0.5% m/m
	BAU	At berth	1	0.04	Fuel sulfur content <= 0.1% m/m
		All other		0.2	Fuel sulfur content <= 0.5% m/m
PM ₁₀	ECA-control	Inside ECA	1	0.11-0.17	Fuel sulfur content <= 0.1% m/m
		Outside ECA		0.48-0.55	Fuel sulfur content <= 0.5% m/m
	BAU	At berth	1	0.11-0.17	Fuel sulfur content <= 0.1% m/m
		All other		0.48-0.55	Fuel sulfur content <= 0.5% m/m
NO _x	ECA-control	Inside ECA	1	0.2-0.25	Ships built after 2025 complying with Tier III
		Outside ECA		0.79-1	All ships complying with Tier II or Tier I
	BAU	At berth	1	0.79-1	All ships complying with Tier II or Tier I
		All other			All ships complying with Tier II or Tier I

³ Based on U.S. EPA (2009), direct PM_{2.5} emission factors are 92% of that of PM₁₀.

2.2 AIR-QUALITY MODELING

The above methods result in two ship emission inventories in 2030, one with and one without the implementation of the ECA policy. To estimate ambient $PM_{2.5}$ and ground-level ozone concentrations in 2030, the geospatial hourly emissions inventory can be aggregated into a spatial resolution consistent with the land-based gridded emissions inventory and fed into an air quality model. We use the regional chemical transport model Weather Research and Forecasting and combine it with Chemistry (WRF-Chem) (Grell et al., 2005) version 3.5 for this purpose. We run it under the scenarios described in Table 3. Comparing the results of Scenario 2 (S2) and Scenario 3 (S3) sheds light on the effectiveness of the ECA policy, and comparing the results of Scenario 1 (S1) and S2 helps us understand the baseline impacts of ship emissions on air quality in 2030.

Table 3. Scenarios and main inputs for air quality modeling

Scenarios	Name	Inputs	Emission control policies for ships
S1	2030 without ship emissions	2030 land emissions	N/A
S2	2030 BAU	2030 land emissions, 2030 baseline ship emissions	SO _x and PM: IMO 2020 global sulfur limit and China national DECA NO _x : IMO Tier II
S3	2030 ECA-control	2030 land emissions, 2030 control ship emissions	SO _x and PM: IMO 2020 global sulfur limit and China 200-nm ECA NO _x : IMO Tier III for ships built after 2025

Our air-quality model used the Regional Acid Deposition Model version 2 (Stockwell, Middleton, Chang, & Tang, 1990) for the gas-phase chemical mechanism to predict the highly nonlinear ozone, sulfate, nitric acid, and hydrogen peroxide concentrations under various atmospheric conditions. For aerosols in the atmosphere, we used the Modal Aerosol Dynamics Model for Europe with the Secondary Organic Aerosol Model (MADE/SORGAM) (Ackermann et al., 1998; Schell et al., 2001). MADE/SORGAM accounts for the aerosol dynamics, including formation (i.e., condensation, nucleation, coagulation), transport, dry deposition, and aerosol-cloud interaction. MADE/SORGAM further predicts the mass of several particulate-phase species, including sulfate, ammonium, nitrate, sea salt, dust, black carbon, organic carbon and secondary organic aerosols in the three log-normal aerosol modes: Aitken, accumulation, and coarse. Photochemistry in the atmosphere was simulated by photolysis of key species. Photolysis rates were obtained from the Fast-J photolysis scheme (Wild, Zhu, & Prather, 2000), which was strongly affected by clouds and aerosols. All meteorological fields and chemical mechanisms stayed the same for both years, 2015 and 2030. More detailed information can be found in the supporting document.

The model simulates ambient $PM_{2.5}$ and ground-level ozone concentrations for the three domains (see Figure 5). The largest domain covers half of Eastern China and some neighboring South Asian countries (36×36 km horizontal grid spacing) and the smallest one covers primarily the GPRD region (4×4 km horizontal grid spacing). The model generates hourly concentrations for every simulation day; those data are then aggregated as a monthly average and used for further analysis. Key inputs and data sources of the model are summarized in Table 4.

Table 4. Key inputs and assumptions to run the WRF-Chem model

Inputs		Data sources/assumptions
Emissions	Ship emissions	Calculated by this paper
	Land emissions	China: 2030 land-based emissions projection by Ma et al. (2017) Outside of China: Representative Concentration Pathway (RCP) 8.5 emission inventory (Riahi et al., 2011)
	Biogenic emissions	Model of Emissions of Gases and Aerosols from Nature version 2.1 (Guenther et al., 2012)
	Dust and sea salt emissions	Calculated online using the dust transport model (Shaw, Allwine, Fritz, Rutz, Rishel, & Chapman, 2008) and sea salt schemes (Gong, 2003)
	Aircraft emissions	Task Force Hemispheric Transport of Air Pollution emissions inventory (Janssens-Maenhout et al., 2015)
Meteorological data	Simulation period	July, due to monsoon season when southeastern winds transport ship emissions from the sea to the land (Lu, Chow, Yao, Fung, & Lau, 2009).
	Meteorological data	Global Forecast System for the year 2015 with 6-h temporal resolution. (National Centers for Environmental Prediction, n.d.; National Centers for Environmental Information, n.d.)

2.3 HEALTH IMPACT ANALYSIS AND VALUATION

Health burdens from ship emissions are estimated by a log-linear model that links changes in air pollution concentrations to health endpoints as follows⁴:

$$\Delta y = y_0 \times Pop \times \left(1 - \frac{1}{e^{\beta} \times (C_1 - C_0)} \right)$$

Where:

β = model parameterized slope of the log-linear relationship between concentration and mortality

Δy = change in premature mortality incidences

y_0 = baseline incidence rate of a given health endpoint

Pop = population

$C_1 - C_0$ = change in air pollution concentration, in $\mu\text{g}/\text{m}^3$

The baseline incidence rate (y_0) for each health endpoint in Guangdong Province and Hong Kong was retrieved from the provincial baseline incidence rate in 2015. We projected to 2030 based on the projected increase in crude death rates from 2015 to 2030 in China, as indicated by the UN Department of Economic and Social Affairs (n.d.). We retrieved the gridded population data for 2015 from the National Aeronautics and Space Administration’s Socioeconomic Data and Applications Center’s fourth version of its Gridded Population of the World (Center for International Earth Science Information Network, 2016). The gridded population data was projected to 2030 based on the methodology developed by the United Nations Department of Economic and Social Affairs (United Nations, Department of Economic and Social Affairs, Population Division, 2017).

⁴ The health endpoints, or diseases, that we consider here include cardiovascular disease, ischemic heart disease, chronic obstructive pulmonary disease, lung cancer, cerebrovascular disease, and respiratory diseases. See the supporting document for more details.

If $C_1 - C_0$ equals the estimated change between S2 and S3, the above equation can calculate the estimated change of health burden due to ECA implementation. Similarly, if $C_1 - C_0$ equals estimated change between S1 and S2, we can get the estimated contribution of ship emissions to various health endpoints in 2030. The remaining task is to estimate β , and that can be calculated as follows:

$$\beta = \frac{\ln(RR)}{\Delta c}$$

Where:

- RR = relative risk, defined as the ratio of death incidence caused by the change of pollution exposure to death incidence among the nonexposed population
- Δc = unit increase in air pollutant concentrations (10 $\mu\text{g}/\text{m}^3$ or 10 parts per billion [ppb])

RR s of $\text{PM}_{2.5}$ -related acute health endpoints are taken from two Pearl River Delta (PRD) specific time series studies (Lin et al., 2016, and Tao et al., 2012). As these RR s only apply to six cities in PRD—Guangzhou, Shenzhen, Dongguan, Foshan, Jiangmen, and Zhuhai—for the health impacts related to acute exposures for this study, we provided mortality estimates for only those six cities.

RR s of $\text{PM}_{2.5}$ -related chronic health endpoints (95% confidence interval) are calculated using the widely adopted integrated exposure-response function developed by Burnett et al. (2014):

$$RR(z) = \begin{cases} 1, & z < z_{cf} \\ 1 + \alpha \{1 - \exp[-\gamma (z - z_{cf})^\delta]\}, & z \geq z_{cf} \end{cases}$$

Where:

- α, γ, δ = model parameters for each health endpoint, decided by fitting a curve to RR data taken from studies on ambient air pollution, secondhand tobacco smoke, household solid cooking fuel, and active smoking
- $RR(z)$ = relative risk at the z exposure level
- z = $\text{PM}_{2.5}$ concentration, in $\mu\text{g}/\text{m}^3$
- z_{cf} = counterfactual concentration below, in which no additional risk is assumed

RR s for ground-level ozone-related chronic health endpoints are taken from a cohort study by Jerrett et al. (2009) that is independent of age groups. The concentration-response relationship for ground-level ozone is:

$$RR = e^{\beta \times (z - z_{cf})}$$

Where:

- β = model parameterized slope of the log-linear relationship between concentration and mortality
- RR = relative risk of ground-level ozone exposure
- z = average 8-hour daily maximum ground-level ozone concentration, in $\mu\text{g}/\text{m}^3$
- z_{cf} = counterfactual concentration below, in which no additional risk is assumed

We used the same concentration-response function to estimate morbidity for hospital admissions and outpatient visits. However, for this it was based on the PM_{10} concentration difference between the 2030 baseline (S2) and control (S3) scenarios and the baseline incidence rates retrieved from Fu et al. (2018), who summarized physician workloads in China from 1998 to 2016. RR s of both hospital admissions and outpatient visits for all ages were obtained from Cao et al. (2009) and Chen et al. (2010),

respectively, who used generalized linear Poisson models to generate the excess risk percentage for a 10 µg/m³ increase of PM₁₀ concentrations.

Finally, we calculated the economic value of avoided mortality by applying the value of statistical life (VSL) method and quantified the economic benefits from reduced morbidity by applying the cost of illness (COI) method. The VSL is the estimated economic value that an average life is worth. The COI estimates pharmaceutical and hospitalization costs and the loss of income during sick leave. Lu, Yao, Fung, and Lin (2016) provided the VSLs and COIs for China from 2010 to 2013 based on the Consumer Price Index in each year. We then projected to 2015 by linear interpolation. The VSL used in this study is \$1.15 million and the COIs for outpatient visits and hospital admissions are \$32.10 and \$1,447.70, respectively (all monetary figures are in 2012 U.S. dollars, unless otherwise indicated). The VSL is likely to grow over time as per capita income increases, and thus our 2030 estimate for the monetized health benefits of an ECA is likely to be conservative.

2.4 COST ANALYSIS

In order to evaluate how much it would cost to reduce SO_x, PM₁₀, and NO_x emissions under an ECA, we estimated the cost effectiveness for shipowners to comply with a 200-nm Chinese ECA in 2030. The cost effectiveness is expressed as dollars per tonne of reduced emissions. The control measures we analyzed to comply with an ECA are as follows.

- » All ships switched to distillate fuel to comply with ECA fuel sulfur limit of 1,000 ppm;
- » All 4-stroke main engines built after 2025 are equipped with selective catalytic reduction (SCR) to comply with Tier III NO_x regulations;
- » All 2-stroke main engines built after 2025 are equipped with exhaust gas recirculation (EGR) to comply with Tier III NO_x regulations; and
- » All 4-stroke auxiliary engines built after 2025 are equipped with SCR regardless of the technology applied to the main engine to comply with Tier III NO_x regulations.

The cost of fuel switching was calculated as follows:

$$C_{fuel\ switching} = FC_{distillate\ fuel} \times P_{distillate\ fuel} - FC_{global\ fuel} \times P_{global\ fuel}$$

Where:

- $C_{fuel\ switching}$ = cost of fuel switching
- $FC_{distillate\ fuel}$ = distillate fuel consumption within ECA, in tonnes
- $P_{distillate\ fuel}$ = distillate fuel price, in \$/tonne
- $FC_{global\ fuel}$ = global marine fuel consumption within ECA, in tonnes
- $P_{global\ fuel}$ = global marine fuel price, in \$/tonne

Fuel consumption was estimated directly using the methods described in Section 2.1. Fuel prices, however, are volatile and difficult to forecast. The cost of fuel switching is largely driven by the price difference between the ECA-compliant fuel (distillate fuel) and the global marine fuel (low-sulfur residual fuel). We use the methods described in Mao and Rutherford (2018a) to estimate high-, medium-, and low-price differentials between the two fuels in 2030. Because fuel switching reduces both SO_x and direct PM₁₀ emissions, we attribute half of the cost to SO_x and half to PM₁₀ (U.S. Environmental Protection Agency [EPA], 2009). The cost effectiveness of a Chinese ECA in reducing

SO_x and PM₁₀ is then calculated by dividing the total attributable cost by the total emissions abated in the entire 200-nm national ECA.

For the cost of Tier III NO_x control technology, we used the cost functions developed in a Danish Economic Impact Assessment (Incentive Partners & Litehauz, 2012) study, as summarized in Table 5. The total cost comprises capital costs (CAPEX), expressed as a function of the engine’s installed power; operational costs related to the usage of the technology; and a slight specific fuel oil consumption (SFOC) increase.

Table 5. NO_x control cost functions

Cost component	EGR (2 stroke)	SCR (4 stroke)
Capital expenditure Y; \$/kW (X: Installed engine power, in MW)	-0.23X + 53.6	0.03X ² -2.07X + 65.1
Operational expenditure; \$/MWh	2.85 (2.3-3.4)	8 (3.1-8.2)
SFOC; g/kWh	0.6	1.5 (1-2)

Note: When there’s a range of values, the applied value reflects the value used in the Danish Economic Impact Assessment study.

In order to capture the cost of Tier III NO_x control technology in 2030, the CAPEX needs to be amortized. We use the following equation to calculate the annualized CAPEX:

$$EAC = C_{initial} \times \frac{r}{1 - (1 + r)^{-p}}$$

Where:

EAC = equivalent annual cost, in \$/year

C_{initial} = initial capital investment, in \$

r = discount rate, or cost of investment

p = number of years for discounting (in this case, a ship’s useful life)

The annualized CAPEX is then modified by a ratio indicating the anticipated time a ship spends in the Chinese ECA versus other ECAs around the world. This is to better reflect the percentage cost of Tier III NO_x control technology that is attributable to the Chinese ECA itself. We sampled AIS data for different OGV ship classes to see how much time a ship travels within different existing ECAs and within the potential Chinese 200-nm ECA. The resulting time ratio spent in a hypothetical Chinese ECA versus existing ECAs is between 0.15 and 1. That is, for every 100 hours spent in all ECAs around the world, including the potential 200-nm Chinese ECA, ships would spend between 15 and 100 hours within the Chinese ECA.⁵ If additional ECAs are implemented by 2030, then this ratio could potentially be lower, and that would result in lower costs attributable to China. The cost effectiveness of the ECA in reducing NO_x emissions is then calculated by dividing the total cost by the total amount of emissions abated in the entire 200-nm Chinese ECA.

⁵ Ships that never appeared in the potential Chinese ECA in 2015 are excluded from sampling.

3. RESULTS AND DISCUSSION

3.1 SHIP EMISSIONS

In Domain 1 (see Figure 5), our study region, we estimated that a total of 122,000 tonnes of SO_x, 195,000 tonnes of NO_x, and 16,600 tonnes of PM₁₀ emissions were emitted by approximately 12,000 OGVs in 2015 (see Table 6). With trade anticipated to grow, we predict that fuel consumption will grow 78% from 2015 to 2030. Thanks to the IMO's 2020 global sulfur limit and China's national DECA, SO_x emissions from OGVs will be cut by nearly two thirds despite the increase in shipping activity under the 2030 BAU scenario. PM₁₀ emissions will be roughly flat (-3%) and NO_x emissions would grow by 67% from 2015 to 2030 under the BAU scenario, mainly due to increased ship activity.

Table 6. Ship emissions within Domain 3, in 2015, 2030 BAU, and 2030 ECA-control scenarios

Pollutant	Emissions (thousand tonnes)			Change in 2030 emissions due to the ECA
	2015	2030 BAU	2030 ECA-control	
SO _x	122	44.4	13.1	-70%
NO _x	195	326	286	-12%
PM ₁₀	16.6	16.1	7.73	-52%

The effectiveness of the ECA policy in reducing SO_x, NO_x, and direct PM₁₀ is evident by comparing emissions under the 2030 BAU and the ECA-control scenarios. SO_x reduction is directly proportional to the 80% decrease in fuel sulfur content from 5,000 ppm to 1,000 ppm. The overall effect, 70%, is less than 80% because cleaner fuels already are required for ships at berth. PM₁₀ emissions are reduced by 52% under the ECA. SO_x emissions fall less than what was estimated by the U.S. EPA in the North American ECA application (U.S. EPA, 2009) due to the implementation of the IMO 2020 global sulfur limit. NO_x emissions drop by 12% because newly built ships make up only a small portion of the fleet between 2025, when we assume the ECA takes effect, and our analysis year of 2030. The effectiveness of the ECA in reducing NO_x emissions will grow over time as more new-build ships become Tier III compliant.

Figure 6 shows how the ECA would affect the distribution of tailpipe NO_x, SO_x, and direct PM₁₀ emissions from ships in the GPRD region. The highest density emissions are in the narrow shipping routes through the Hong Kong islands and the Pearl River estuary, which lead to inland river ports, and these emissions significantly impact nearby communities. An ECA would reduce emissions, improve air quality, and benefit human health in those areas, as explained in the following sections.

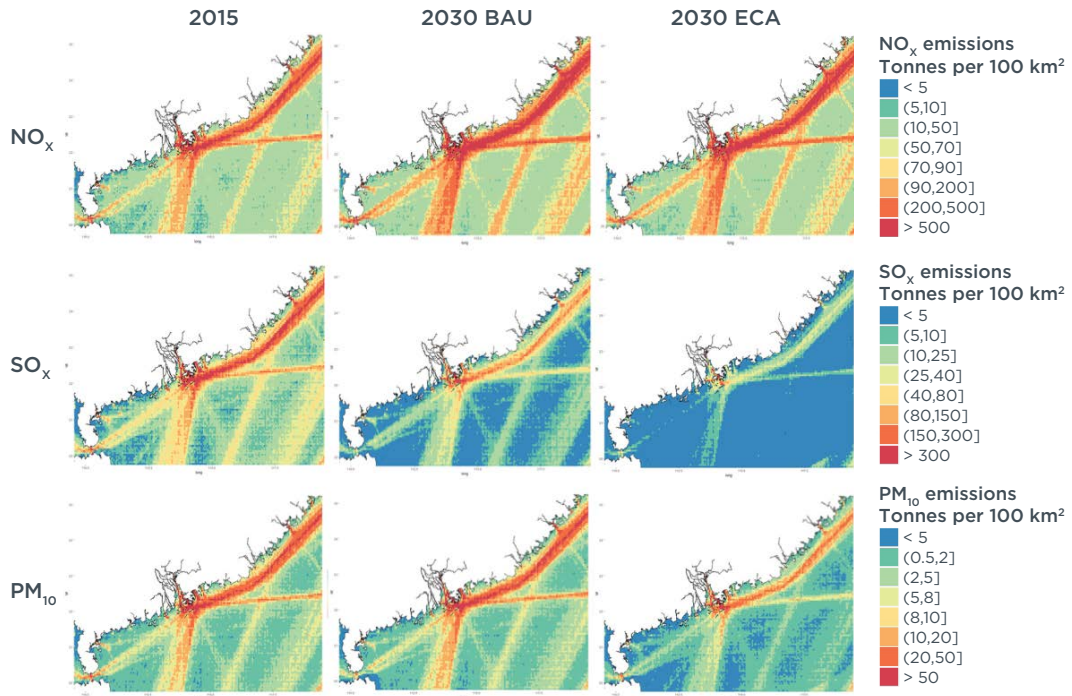


Figure 6. Distribution of NO_x, SO_x, and PM₁₀ tailpipe emissions from ships in 2015 and 2030, BAU versus with an ECA.

3.2 AIR QUALITY

Compared to 2015, the relative contribution of ship emissions to ambient PM_{2.5} and ozone emissions increases in 2030 as land-based emissions drop over the same period. The ECA policy would help in reducing the level of impact, which differs by geographical location. Table 7 summarizes the simulation results from the WRF-Chem model in GPRD cities.

Table 7. Shipping contribution to PM_{2.5} and ozone concentrations and ECA effectiveness in 2030 in GPRD cities

Pollutants	Cities	Shipping contribution $\mu\text{g}/\text{m}^3$ (%)			Change due to the ECA $\mu\text{g}/\text{m}^3$ (%)
		2015	2030 BAU	2030 ECA	
PM _{2.5}	Guangzhou	2.15 (2.90%)	2.30 (12.9%)	1.61 (9.20%)	-0.69 (-3.88%)
	Dongguan	1.06 (1.40%)	2.85 (19.2%)	2.07 (14.7%)	-0.78 (-5.23%)
	Foshan	1.66 (2.30%)	0.84 (5.49%)	0.35 (2.36%)	-0.49 (-3.20%)
	Hong Kong	6.12 (11.97%)	3.56 (34.1%)	2.07 (22.4%)	-1.49 (-13.9%)
	Huizhou	2.3 (7.30%)	3.1 (21.0%)	1.68 (12.1%)	-1.42 (-9.27%)
	Jiangmen	1.06 (3.30%)	-0.13 (-1.42%)	0.21 (2.22%)	+0.34 (+3.72%)
	Shenzhen	4.01 (4.20%)	3.41 (27.4%)	2.33 (21.0%)	-1.08 (-8.56%)
	Zhaoqing	0.11 (0.40%)	0.19 (2.03%)	-0.43 (-4.93%)	-0.62 (-6.63%)
	Zhongshan	0 (0%)	-0.13 (-1.06%)	0.03 (<1%)	+0.16 (+1.31%)
	Zhuhai (&Macao)	1.4 (3.80%)	0.23 (2.21%)	0.08 (<1%)	-0.15 (-1.44%)
	GPRD	1.43 (3.25%)	1.48 (12.0%)	1.20 (9.95%)	-0.28 (-2.28%)
Ozone	Guangzhou	1.65 (2.80%)	1.62 (3.87%)	1.27 (3.06%)	-0.35 (< -1%)
	Dongguan	1.46 (2.50%)	3.15 (7.65%)	2.63 (6.47%)	-0.52 (-1.26%)
	Foshan	1.76 (3.00%)	2.17 (5.24%)	2.18 (5.26%)	+0.01 (< +1%)
	Hong Kong	5.80 (11.96%)	6.09 (15.2%)	5.8 (14.6%)	-0.29 (< -1%)
	Huizhou	2.75 (5.20%)	3.69 (9.36%)	3.09 (7.96%)	-0.60 (-1.52%)
	Jiangmen	1.86 (3.60%)	3.19 (8.54%)	3.34 (8.90%)	+0.15 (+0.40%)
	Shenzhen	3.5 (6.30%)	4.84 (12.0%)	4.4 (11.0%)	-0.44 (-1.09%)
	Zhaoqing	0.72 (1.50%)	0.85 (2.43%)	1.18 (3.35%)	+0.33 (+0.94%)
	Zhongshan	2.54 (4.37%)	3.94 (9.57%)	3.49 (8.57%)	-0.45 (-1.09%)
	Zhuhai (&Macao)	4.22 (7.80%)	5.19 (13.2%)	4.94 (12.7%)	-0.25 (< -1%)
	GPRD	1.90 (3.71%)	2.59 (6.72%)	2.47 (6.43%)	-0.12 (< -1%)

Over the 15 years analyzed, the ambient PM_{2.5} concentration in the GPRD region is expected to drop from 32.4 $\mu\text{g}/\text{m}^3$ to 12.32 $\mu\text{g}/\text{m}^3$, mainly due to large reductions of PM_{2.5} precursors from land-based sources. Over the same time period, ships' contribution to ambient PM_{2.5} concentration increases by 0.05 $\mu\text{g}/\text{m}^3$, and from 3.25% to 12.0%, on average. If an ECA were implemented, the average PM_{2.5} concentration would fall from 12.32 $\mu\text{g}/\text{m}^3$ to 12.04 $\mu\text{g}/\text{m}^3$ within GPRD in 2030, a 2.3% decrease. Although the overall PM_{2.5} reduction may seem small, the city-level PM_{2.5} concentration reductions are noteworthy. We predict reductions in 2030 ambient PM_{2.5} concentrations of about 14% in Hong Kong, 9% in Shenzhen, and 9% in Huizhou as a result of the ECA. Shenzhen and Hong Kong are two of most developed and populated cities in the GPRD region, and

each is expected to have more than 25 million residents by 2030. Thus, an ECA would improve air quality for a substantial number of people.⁶

Ozone reductions are more subtle. In the GPRD region between 2015 and 2030, ground-level ozone concentration drops from 50.6 ppb to 38.5 ppb, while ships' contribution to ground-level ozone increases from 3.2% to 6.7%. At the city level in 2030, six out of 11 GPRD cities (Shenzhen, Zhuhai, Hong Kong, Jiangmen, Huizhou, and Zhongshan) are expected to have around 10% (between 8.5% and 13.2%) of ground-level ozone linked to shipping. An ECA would reduce ground-level ozone concentration by about 0.12 ppb, a less than 1% reduction from the 2030 BAU scenario. Again, the city-level reduction rates are more noteworthy, and the largest reduction is 1.52% in Huizhou. Overall, the ozone reduction due to ECA implementation is smaller compared to the PM_{2.5} reduction. These ozone reductions, while small, are nevertheless expected to result in health benefits, as we describe in the next section.

3.3 HEALTH BENEFITS

Enacting a 200-nm wide Chinese ECA would yield substantial health benefits. In 2030, an ECA would prevent about 1,431 premature deaths (mortality) in GPRD cities. That is a 23% reduction from BAU and equivalent to about \$1.65 billion in economic benefits (see Table 8). Most of the ECA health benefits are due to reduced PM_{2.5}-related chronic mortality (83.3%).⁷ Although the effectiveness of the ECA in preventing acute mortality caused by PM_{2.5} outweighs that of ozone (25% versus 11%), the actual number of lives saved by ozone reduction is higher (43 versus 35).

Table 8. Expected health and economic benefits in 2030 from an ECA in the GPRD region

Health effect			2030 BAU ship-related incidence	2030 ECA change	ECA relative change	Economic benefits (millions of dollars)
Premature mortality	PM _{2.5} -related	Acute mortality	142	-35	-25%	40
		Chronic mortality	4,033	-1,193	-30%	1,376
	ozone-related	Acute mortality	380	-43	-11%	50
		Chronic mortality	1,738	-160	-9%	184
Morbidity	PM ₁₀ -related	Hospital admissions	—	-1,714	—	3
		Outpatient visits	—	-38,327	—	1
Grand Total						1,654

Note: All numbers are rounded to integers and are taken as the midpoint of a confidence range.

3.3.1. Premature mortality associated with PM_{2.5} exposure

PM_{2.5} pollution causes early deaths due to acute and chronic health problems. The tables below show acute (Table 9) and chronic (Table 10) premature mortality due to ship-related PM_{2.5} in the GPRD cities, and the effectiveness of an ECA in reducing those effects.

6 Note that the model identified a few places where ECA implementation would increase, rather than decrease, PM_{2.5} and ozone concentrations. This is because WRF-Chem is an “online” regional coupled model with feedbacks enabled between the weather and chemistry components of the model. It allows a two-way interaction between the aerosol, radiation, and cloud processes (Grell & Baklanov, 2011) that can affect pollution concentrations in nonlinear ways. The overall air quality impacts of the ECA are overwhelmingly positive.

7 Chronic mortality refers to deaths due to diseases like ischemic heart disease, chronic obstructive pulmonary disease, lung cancer, and cerebrovascular disease.

Table 9. BAU and ECA-reduced premature mortality associated with acute exposure to ship-related PM_{2.5} in 2030

City	2030 BAU ship-related incidence	2030 ECA change	ECA relative change
Guangzhou	63 (52, 73)	-8 (-6, -9)	-13%
Shenzhen	23 (19, 27)	-8 (-7, -10)	-35%
Dongguan	23 (19, 27)	-6 (-5, -7)	-26%
Foshan	15 (13, 18)	-12 (-10, -14)	-80%
Jiangmen	12 (10, 14)	1 (1, 1)	+8%
Zhuhai	6 (5, 7)	-2 (-2, -2)	-33%
Six-city total	142 (118, 166)	-35 (-29, -41)	-25%

As shown in Table 9, in 2030, BAU ship-related PM_{2.5} is expected to cause a total of 142 acute premature deaths in the six cities from all health endpoints. Among those, cardiovascular disease accounts for 77 incidences and respiratory disease accounts for 17 incidences. (A detailed summary by disease can be found in the supporting document.) Guangzhou, Shenzhen, and Dongguan seem to suffer the most (more than 20 incidences each) and Guangzhou alone would experience 63 acute premature deaths due to ship-related PM_{2.5} pollution. The ECA would reduce 35 deaths in the six cities from all health endpoints, with an overall reduction rate of nearly 25% compared to the BAU scenario.

The ECA is even more effective in reducing PM_{2.5}-related chronic premature deaths (see Table 10). Among the GPRD cities, Shenzhen would suffer the most from ship-induced PM_{2.5} pollution in 2030, with an estimated 980 chronic premature deaths occurring under the BAU scenario from all health endpoints. Guangzhou, Dongguan, Huizhou, and Hong Kong would also incur more than 500 chronic premature deaths in 2030 due to ship-induced PM_{2.5}. With the 200-nm ECA, nearly 1,200 of those deaths could be avoided—a 30% reduction compared to the BAU scenario. This is equivalent to a monetized value of around \$1.4 billion that year.

Table 10. BAU and ECA-reduced premature mortality associated with chronic exposure to ship-related PM_{2.5} in 2030.

City	2030 BAU ship-related incidence	2030 ECA change	ECA relative change
Guangzhou	641 (235, 1019)	-82 (-28, -131)	-13%
Shenzhen	980 (405, 1367)	-356 (-147, -496)	-36%
Foshan	227 (85, 357)	-178 (-67, -281)	-78%
Zhuhai (&Macao) ^a	117 (49, 162)	-33 (-14, -46)	-28%
Jiangmen	90 (37, 127)	+11 (+4, +14)	+12%
Dongguan	653 (255, 999)	-179 (-72, -265)	-27%
Zhaoqing	27 (11, 38)	-25 (-10, -33)	-93%
Huizhou	571 (235, 877)	-162 (-66, -250)	-28%
Zhongshan	85 (35, 122)	+16 (-7, -23)	+19%
Hong Kong	642 (201, 948)	-205 (-64, -303)	-32%
Total	4,033 (1,548, 6016)	-1,193 (-457, -1,768)	-30%

The results for Zhuhai include Macao. Because Macao is a very small region, it falls into the same grid cell as Zhuhai in our finest model resolution (4 x 4 km).

Figure 7 illustrates the distribution of health benefits from PM_{2.5} reduction by the ECA policy throughout the GPRD. Even though ship emissions are concentrated near the coastline and within the Pearl River Delta, the impacts are spread widely inland. Accordingly, even though the ECA policy only covers the sea portion of the GPRD region, its benefits also spread inland, especially around the highly-populated Guangzhou and Foshan areas.

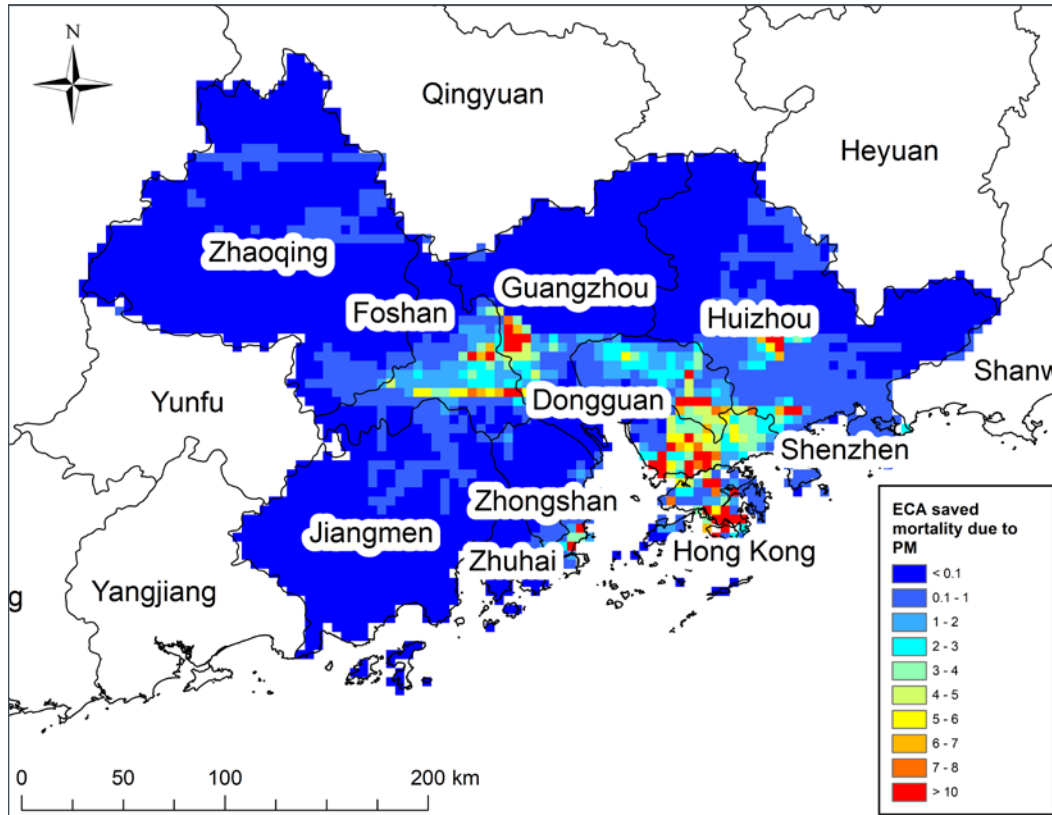


Figure 7. Distribution of avoided PM_{2.5} chronic mortality in 2030 due to ECA controls.

3.3.2. Premature mortality associated with ozone exposure

Similar to PM_{2.5}, ground-level ozone pollution would lead to acute and chronic illness and cause premature deaths. The tables below detail the acute (Table 11) and chronic (Table 12) effects of ship-induced ozone on premature deaths in GPRD cities, and include the reductions linked to the ECA.

Table 11. BAU and ECA-reduced premature mortality associated with acute exposure to ship-related ozone in 2030

City	2030 BAU ship-related incidence	2030 ECA change	ECA relative change
Guangzhou	127 (99, 157)	-27 (-21, -33)	-21%
Shenzhen	52 (40, 64)	-3 (-2, -4)	-6%
Dongguan	35 (27, 43)	-6 (-5, -7)	-17%
Foshan	50 (39, 62)	-6 (-4, -7)	-12%
Jiangmen	90 (70, 111)	0 (0, 0)	0%
Zhuhai	26 (20, 32)	-1 (-1, -2)	-4%
Total	380 (295, 469)	-43 (-33, -53)	-11%

Table 12. BAU and ECA-reduced premature mortality associated with chronic exposure to ship-related ozone in 2030

City	2030 BAU ship-related incidence	2030 ECA change	ECA relative change
Guangzhou	238 (67, 479)	-50 (14, 101)	-21%
Shenzhen	303 (86, 607)	-18 (-5, -36)	-6%
Foshan	136 (38, 272)	-15 (-4, -30)	-11%
Zhuhai (&Macao)	67 (19, 134)	-4 (-1, -8)	-6%
Jiangmen	97 (27, 194)	0 (0, 0)	0%
Dongguan	171 (48, 342)	-30 (-8, -60)	-18%
Zhaoqing	26 (7, 52)	+12 (+3, +24)	+46%
Huizhou	144 (41, 289)	-24 (-7, -48)	-17%
Zhongshan	83 (23, 166)	-10 (-3, -20)	-12%
Hong Kong	473 (144, 875)	-21 (-6, -39)	-4%
Total	1,738 (500, 3,410)	-160 (-45, -318)	-9%

Relative to $PM_{2.5}$, the ECA's impact on ship-induced premature deaths due to ozone exposure is smaller, but still significant. Table 11 shows that four of the six cities could incur more than 50 premature deaths due to acute ozone exposure due to ships under the BAU scenario. The ECA policy would reduce those incidences by up to 21%, and Guangzhou would benefit the most. Overall, the 200-nm ECA could avoid around 200 premature deaths due to ship-related ozone exposure. That is a 10% reduction from BAU. The monetized value of these benefits is estimated at about \$0.23 billion. Figure 8 helps illustrate how these health effects are distributed across GPRD cities. Similar to Figure 7, significant benefits accrue inland.

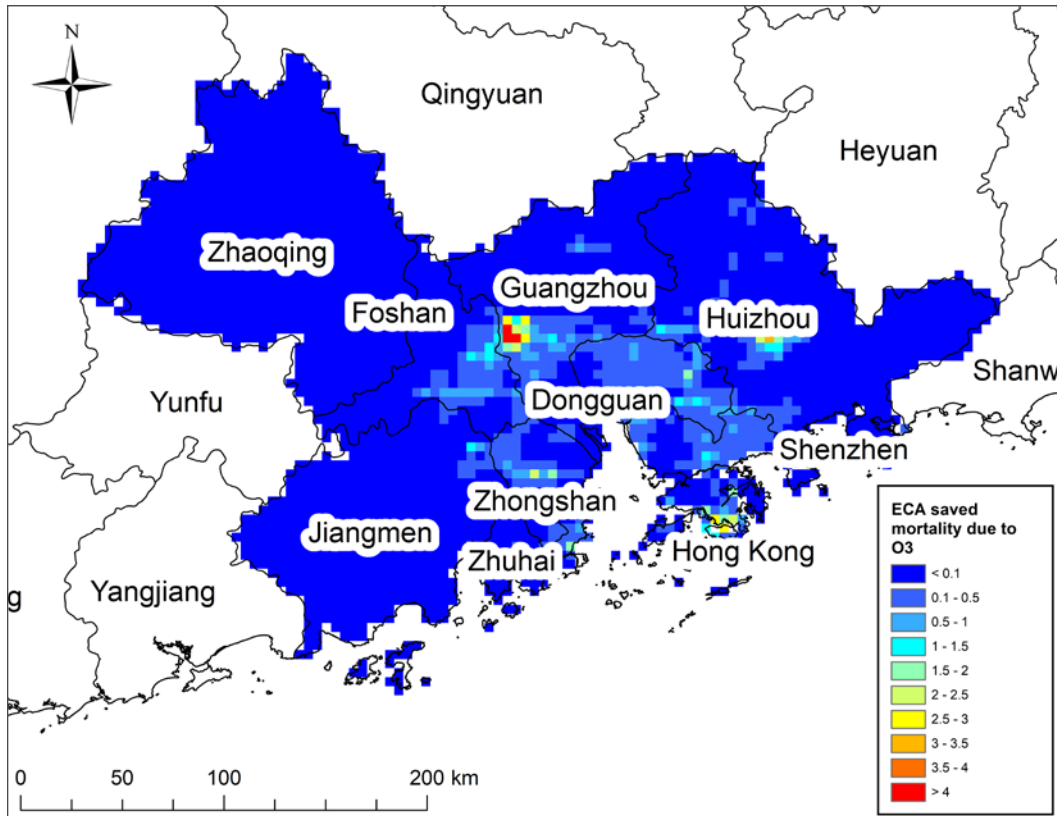


Figure 8. Distribution of avoided ozone chronic mortality in 2030 due to ECA controls.

3.3.3. Reduced morbidity associated with ECA policy

Air pollution results not only in lost lives, but also in additional hospital visits. In 2030, reduced ambient PM₁₀ concentrations (from 15.60 µg/m³ to 15.39 µg/m³) from a Chinese ECA would be expected to avoid more than 38,000 outpatient visits and 1,700 hospital admissions in the GPRD. The monetized benefits, although dwarfed by the saved lives, amount to about \$4 million based on the associated COI values.

Table 13. ECA-reduced morbidity in the GPRD region due to reduced PM₁₀ concentration.

City	Hospital admissions	Outpatient visits
Guangzhou	-71 (60, -206)	-1,597 (436, -3,772)
Shenzhen	-498 (416, -1,436)	-11,135 (3,039, -26,297)
Foshan	-286 (238, -823)	-6,386 (1,743, -15,081)
Zhuhai (& Macao)	-49 (41, -141)	-1,097 (299, -2,591)
Jiangmen	35 (-29, 101)	782 (-213, 1,847)
Dongguan	-262 (219, -755)	-5,855 (1,598, -13,827)
Zhaoqing	-20 (17, -58)	-451 (123, -1,066)
Huizhou	-315 (263, -909)	-7,052 (1,925, -16,655)
Zhongshan	48 (-40, 140)	1,082 (-295, 2,556)
Hong Kong	-296 (247, -853)	-6,618 (1,806, -15,630)
Total	-1,714 (1,432, -4,940)	-38,327 (10,461, -90,516)

3.4 COSTS TO SHIPOWNERS

3.4.1. Cost effectiveness of the ECA compared to similar studies

With different fuel price differential assumptions, we estimate that the entire Chinese 200-nm ECA would incur a total cost of \$2.2 billion due to switching to cleaner, more expensive distillate fuel. Assuming that half of these costs can be attributed to SO_x emission reduction and half to PM₁₀, the cost-effectiveness of enacting a 200-nm ECA in China would be \$4,400 per tonne for SO_x and \$16,000 per tonne for PM₁₀.

These results can be compared with similar studies. Table 14 lists the cost-effectiveness of China's power plant desulfurization devices and for existing and prospective ECA applications.⁸ The results of this study are reasonably in line with other estimates after taking into account differences in the underlying methodologies. Calculations of the cost effectiveness of ECAs are highly sensitive to assumptions about baseline fuel quality: It was 2.5% m/m for the North American ECA, 1.5% for the Mediterranean ECA (Rouil, Ratsivalaka, André, & Allemand 2019), and we assumed 0.5% for this study, given the 2020 global fuel sulfur limit.

Table 14. Cost-effectiveness of fuel-switching for ECA compliance compared to other sulfur control programs

Programs	Cost applicable year	Annual SO _x cost/tonne	Annual PM ₁₀ cost/tonne
China coal-fired power plant desulfurization program	2010-2015	\$200-\$227	—
200-nm Chinese ECA	2030	\$4,400	\$16,000
North America ECA	2020	\$1,367	\$11,400
Mediterranean ECA	2015	\$2,620-\$3,560	—

The desulfurization cost for China's coal-fired power plants is listed here as a reference in Table 14. We caution that the cost relates to running scrubbers, something that is not evaluated as an ECA compliance option for ships in this study. Additionally, the scrubbers were manufactured locally, and they are usually much cheaper than their western counterparts.

The Tier III compliant ships will incur both capital costs and operational costs. In 2030, we estimated that these ships would incur an amortized capital cost of \$105 million within the entire Chinese ECA. The operational cost, on the other hand, is a recurring cost depending on the usage of NO_x control technologies, mainly urea use for SCR systems (Incentive Partners & Litehauz, 2012). The fuel penalty associated with the EGR technology is also considered as an operational cost because it impacts fuel efficiency. That operational cost is estimated at \$97 million for the entire Chinese ECA in 2030. Altogether, the annualized cost of Tier III NO_x control measures for the 200-nm Chinese ECA is estimated at \$202 million, which translates to cost effectiveness of \$638 per tonne.

These absolute costs are relatively low because ships only need to be Tier III compliant starting in 2025. With our fleet turnover model (see Section 2.1.2), about 13% of the fleet will be NO_x compliant in 2030. In reality, this could be even lower. That is because

⁸ The cost for the Mediterranean ECA is expressed in 2016 Euros. We converted it to 2012 U.S. dollars for the comparison in Table 14.

shipowners know when to expect ECA regulations and typically speed up new ship construction before that date. This was already observed when there was an unusual peak of new-build ship orders in December 2015, in anticipation of the start of the Tier III regulations for the North American ECA in January 2016.

However, the existing ECAs potentially will have a spillover effect on future ECAs. Certain ships traveling to existing ECAs are already Tier III compliant, and if they also travel in the future Chinese ECA, they might choose to operate at Tier III-level NO_x emissions, even if they were built before 2025. Still, we anticipate this spillover effect will be mostly negligible, because (1) a small number of new ships will need to comply with Tier III standards in existing ECAs and (2) most of them will install SCR and EGR equipment, which can be turned on and off (U.S. EPA, 2009).

We also can compare the cost-effectiveness of Tier III NO_x compliance of the Chinese ECA with similar pollution control programs (see Table 15).⁹ Our results are lower than previous ECA studies, and this reflects how ships operating globally can split NO_x aftertreatment capital costs across multiple ECAs. Additionally, the North American ECA’s result includes engine upgrade cost from Tier I to Tier II, whereas the majority of ships in this study are already Tier II compliant.

Table 15. Cost effectiveness of ECA Tier III NO_x compliance compared to other NO_x control programs

Programs	Time frame	Annual NO _x cost/tonne
China coal-fired power plant denitration program	2010–2015	\$606–\$768
200-nm Chinese ECA	2030	\$638
North American ECA	2020	\$2,960
North Sea NECA	2030	\$2,048
Baltic Sea NECA	2030	\$1,165–\$1,553
Mediterranean ECA	2015	\$1,370–\$1,520

As described in Section 2.4, cost estimation is based on assumptions with considerable uncertainty, particularly fuel costs in 2030. We performed a sensitivity analysis to investigate how variation in input values affect our cost results. The results are summarized in Table 16, which reflects variable assumptions on fuel price differential, discount rate, ships’ longevity, and capital cost of Tier III compliance technology. Further details can be found in the Appendix.

Table 16. Cost analysis results from the sensitivity analysis

Cost item	Cost range	Medium cost used in the main analysis
Total cost of fuel switching, entire China ECA	\$0.73 billion to \$3.7 billion	\$2.2 billion
Total cost of NO _x abatement, entire China ECA	\$153 million to \$247 million	\$202 million
Cost per tonne of SO _x abatement	\$1,400–\$7,300	\$4,400
Cost per tonne of NO _x abatement	\$483–\$781	\$638
Cost per tonne of PM ₁₀ abatement	\$5,300–\$27,000	\$16,000

⁹ The cost for the Mediterranean ECA is expressed in 2016 euros. We converted it to 2012 U.S. dollars for the comparison in Table 15.

3.4.2. Net benefits and benefit-cost ratio of the ECA policy in the GPRD region

The results discussed above are for the entire Chinese ECA, not just for the GPRD. In order to directly compare the monetized health benefits of the ECA with the costs to ships operating in the region, we drew two boundaries (see Figure 9) for geofencing the national emissions inventory. This is both consistent with a previous ICCT publication for OGV emissions in the same region (Mao et al., 2017) and corresponds to the 11 GPRD cities we analyzed for health benefits. This approach is needed because the atmosphere is a homogeneous system and no absolute boundary can be drawn to reflect air quality improvement solely in the GPRD region.

Figure 9 shows the study region, the existing GPRD DECA (green wedge), and the hypothetical 200-nm IMO-designated Chinese ECA (blue). To determine which portion of overall compliance costs should be assigned to the GPRD region, two zones within the ECA are defined by the dotted white lines. The rectangular dotted line boundary is the smaller emission boundary and captures an optimistic estimate of the total costs. The larger one, the semi-circle emission boundary (200-nm radius), is a conservatively high estimate.

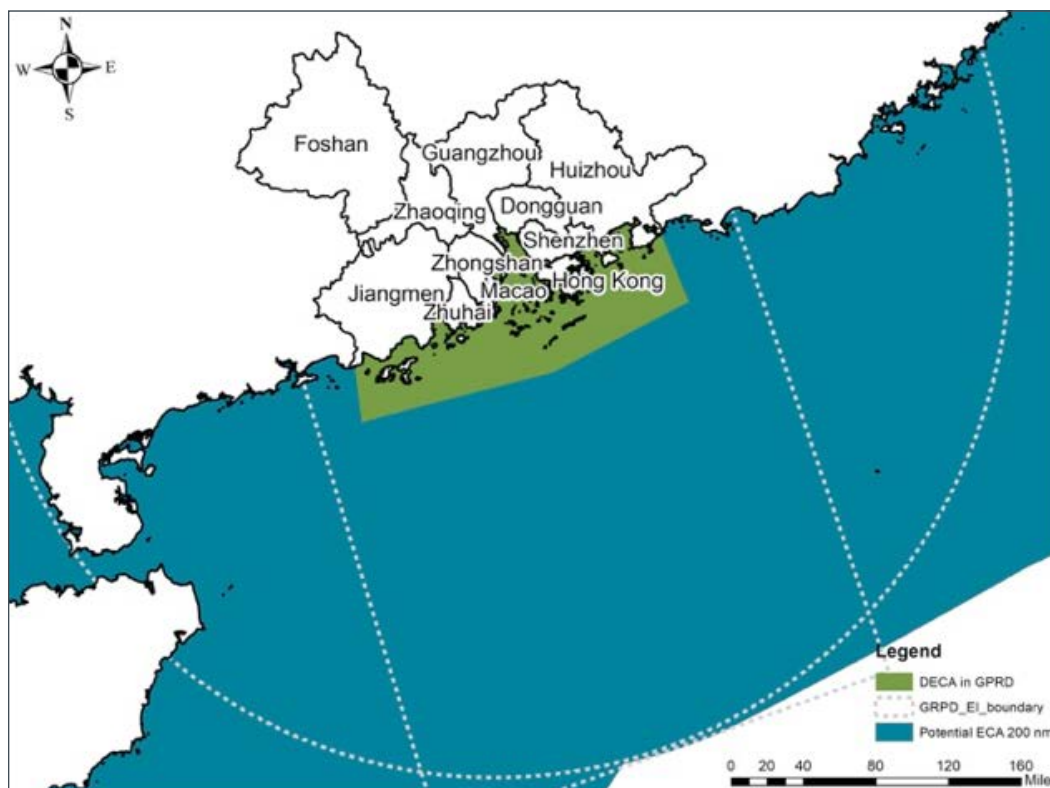


Figure 9. Cost analysis boundaries for the GPRD region.

Within the smaller emission inventory boundary, we estimated that a 200-nm ECA would reduce 29,400 tonnes of SO_x , 7,910 tonnes of PM_{10} , and 38,000 tonnes of NO_x . This corresponds with a total cost of fuel switching in the GPRD region of \$258 million and around \$24 million to comply with Tier III NO_x standards. This adds up to a total cost of ECA compliance in the GPRD region of \$282 million, which corresponds to a net benefit of \$1.372 billion and a benefit-cost ratio of about 6:1.

The larger, semicircle emission inventory boundary would result in proportionally higher emission reductions for all three pollutants (44,000 tonnes of SO_x , 12,000 tonnes of

PM₁₀, and 57,000 tonnes of NO_x), and a higher cost of ECA compliance. We estimated that the total fuel switching cost in the GPRD region is \$389 million and it costs around \$37 million to comply with Tier III NO_x standards. The total cost of ECA compliance in the GPRD region is thus estimated at \$426 million, which corresponds to a smaller net benefit of \$1.226 billion and a smaller benefit-cost ratio of about 4:1. These costs are shown as a bar chart (Figure 10) and graphically (Figure 11).

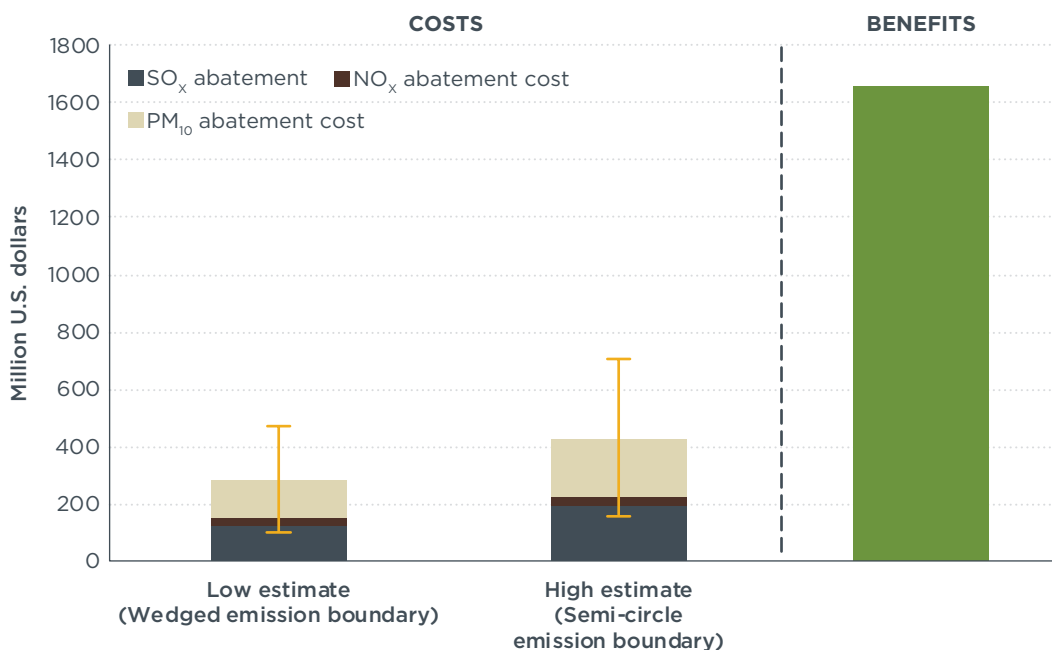


Figure 10. Costs and benefits of a 200-nm ECA in the GPRD region.

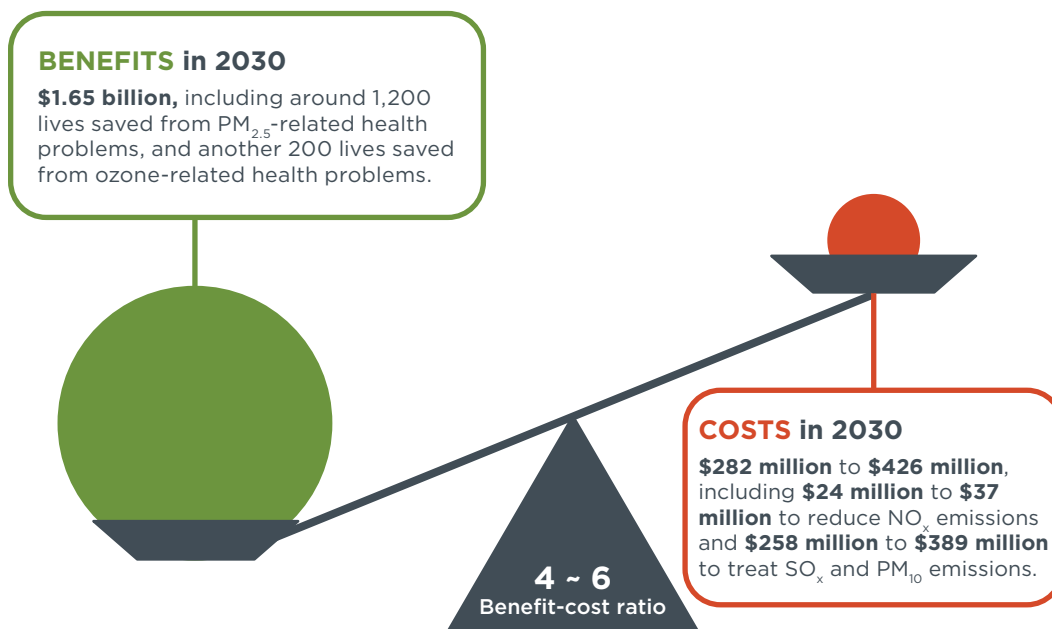


Figure 11. Benefit-cost ratio for the GPRD region from a 200-nm Chinese ECA.

Our sensitivity analysis also provides a range of the above values, summarized in Table 17.

Table 17. Benefits and costs analysis for the GPRD region from the sensitivity analysis

Emission boundary	Evaluation items	Range	Medium value used in the main analysis
Wedge boundary	Total cost of fuel switching, GPRD	\$85 million to \$431 million	\$258 million
	Total cost of NO _x abatement, GPRD	\$18 million to \$29 million	\$24 million
	Net benefits	\$1.19 billion to \$1.55 billion	\$1.37 billion
	Benefit-cost ratio	3.6-16	6:1
Semi-circle boundary	Total cost of fuel switching, GPRD	\$128 million to \$651 million	\$389 million
	Total cost of NO _x abatement, GPRD	\$28 million to \$45 million	\$37 million
	Net benefits	\$0.96 billion to \$1.50 billion	\$1.23 billion
	Benefit-cost ratio	2.4-10.5	4:1

To put this benefit-cost ratio into perspective, we can compare it with other emission control policies. As detailed in the Air Pollution Action Plan released in 2013, the Chinese government plans to aggressively regulate air pollution from industry, transportation, and construction.¹⁰ Although benefit-cost ratios from specific initiatives of this Action Plan are not publicly available, the ICCT has been evaluating China's motor vehicle emission control programs for years and has made estimates of associated costs and benefits (Shao & Wagner, 2015). The evaluated programs have positive benefit-cost ratios that are expected to become more positive over the years.

Figure 11 presents the annual costs and benefits of regulating China's motor vehicles evaluated over 30 years (2015–2045). The green line, which indicates the net benefit, grows consistently and would reach about 50 billion renminbi in 2030. This is a benefit-cost ratio of approximately 2:1 in 2030 and is smaller than that of the ECA policy in the GPRD region.¹¹

¹⁰ A five-year action plan for a series of aggressive actions to fight against air pollution. Please see official document here: http://www.gov.cn/zwqk/2013-09/12/content_2486773.htm

¹¹ Methodological differences between this report and Shao and Wagner (2015) could explain some of the differences in the estimated benefit-cost ratio. The 2015 report likely underestimated the total health benefits because it did not account for all diseases included in this study, leading to a conservative benefit-cost ratio.

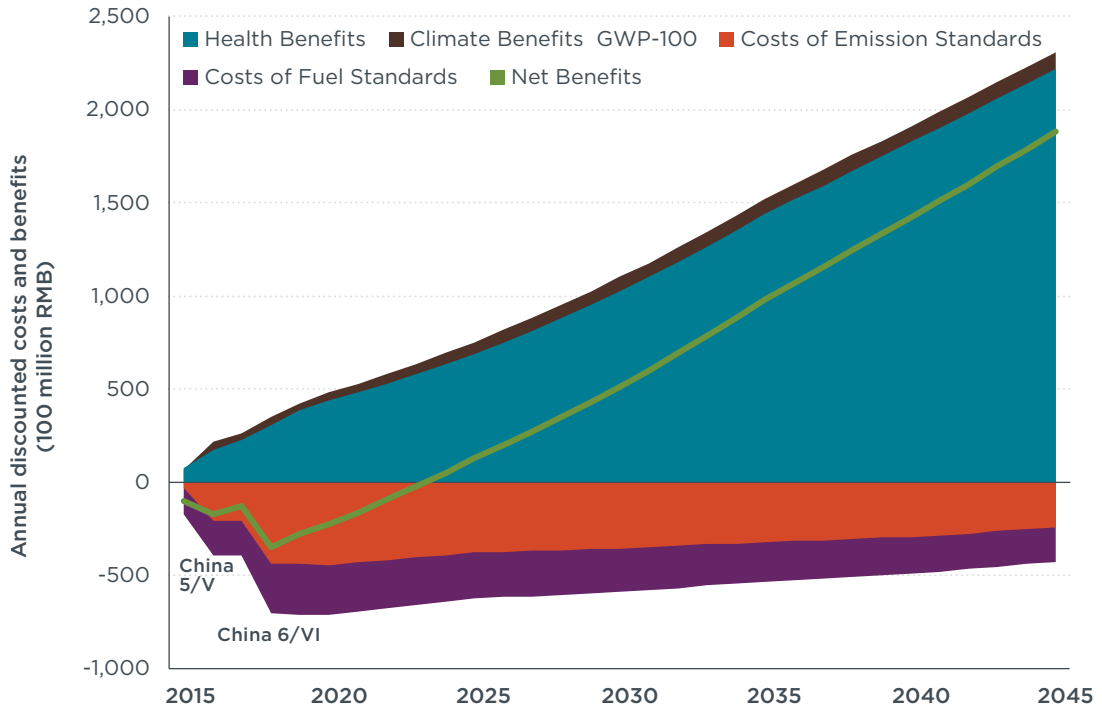


Figure 12. Annual discounted costs and benefits of national motor vehicle emission control programs in China, 2015–2045 (Shao & Wagner, 2015).

4. CONCLUSIONS

In this paper, we estimated the costs and benefits of an IMO-designated ECA in China's GPRD region in 2030 and compared its cost effectiveness with air pollution control policies targeting land-based sources. We assumed an ECA that is 200-nm wide, in place by 2025, and that it requires both fuel-quality improvements to reduce SO_x and PM and more stringent, Tier III NO_x requirements for engines on ships built in 2025 or later.

Based on the SAVE model and 2015 AIS data, we estimated ship emissions in 2015 and projected them out to 2030. The results show that an ECA could cut SO_x, PM₁₀, and NO_x emissions by 70%, 52%, and 12%, respectively, in the GPRD region in 2030 compared to a BAU scenario. This would reduce ambient PM_{2.5} concentrations in 2030 by more than 10% in major port cities like Shenzhen and Hong Kong and produce a smaller reduction (1%) in ozone concentration, when compared to the 2030 BAU scenario.

Our results suggest that an ECA would avoid about 1,400 premature deaths, 1,700 hospital admissions, and 38,000 outpatient visits per year in the GPRD region in 2030. This avoided mortality and morbidity translates to nearly \$1.65 billion in annual benefits in 2030. As a point of comparison, the U.S. EPA estimated that the North American ECA could avoid between 3,800 and 9,500 premature deaths in 2020 for the entire United States, based mainly on reducing the fuel sulfur content from an average of 25,000 ppm to 1,000 ppm. In the GPRD region alone, based on a much smaller fuel quality improvement (5,000 ppm sulfur) and a similar 5-year introduction of Tier III engines, an ECA could avoid up to about one-third as many deaths as the 200-nm North American ECA avoids each year.

Regarding the cost effectiveness of reducing SO_x, PM₁₀, and NO_x emissions via a Chinese ECA, we estimated that it would cost about \$4,400 to avoid one tonne of SO_x emissions in 2030. One tonne of direct PM₁₀ abated would cost about \$16,000 and mitigating one tonne of NO_x emissions would cost another \$638. In all, the ECA policy was estimated to cost between \$282 million and \$426 million in 2030, with associated benefits of about \$1.65 billion in the GPRD region. This results in benefit-cost ratios ranging from 4:1 to 6:1. The benefit-cost ratios are comparable to, and in some cases superior to, land-based controls.

These results suggest that a Chinese international ECA would lead to substantial air quality and public health benefits. Now that China has upgraded its national DECA, applying for an IMO-designated ECA may be an appropriate next step to further protect its coastal communities from shipping air pollution.

REFERENCES

- Ackermann, I. J., Hass, H., Memmesheimer, M., Ebel, A., Binkowski, F. S., & Shankar, U. (1998). Modal aerosol dynamics model for Europe: Development and first applications. *Atmospheric Environment*, *32*(17), 2981–2999. doi:10.1016/S1352-2310(98)00006-5
- Anenberg, S., Miller, J., Henze, D., & Minjares, R. (2019). *A global snapshot of the air pollution-related health impacts of transportation sector emissions in 2010 and 2015*. Retrieved from the International Council on Clean Transportation, <https://www.theicct.org/publications/health-impacts-transport-emissions-2010-2015>
- Boylan, J. W., & Russell, A. G. (2006). PM and light extinction model performance metrics, goals, and criteria for three-dimensional air quality models. *Atmospheric Environment*, *40*(26), 4946–4959, doi: 10.1016/j.atmosenv.2005.09.087
- Burnett, R. T., Pope, C. A., Ezzati, M., Olives, C., Lim, S. S., Mehta, S., ... Cohen, A. (2014). An integrated risk function for estimating the global burden of disease attributable to ambient fine particulate matter exposure. *Environmental Health Perspectives*, *122*(4), 397–403. doi:10.1289/ehp.1307049
- Cao, J., Li, W., Tan, J., Song, W., Xu, X., Jiang, C., ... & Kan, H. (2009). Association of ambient air pollution with hospital outpatient and emergency room visits in Shanghai, China. *Science of The Total Environment*, *407*(21), 5531–5536. doi:10.1016/j.scitotenv.2009.07.021
- Center for International Earth Science Information Network - CIESIN - Columbia University. (2016). Gridded Population of the World, Version 4 (GPWv4): Administrative Unit Center Points with Population Estimates. Palisades, NY: NASA Socioeconomic Data and Applications Center (SEDAC). doi:10.7927/H4F47M2C.
- Chen, R., Chu, C., Tan, J., Cao, J., Song, W., Xu, X., ... Kan, H. (2010). Ambient air pollution and hospital admission in Shanghai, China. *Journal of Hazardous Materials*, *181*(1-3), 234–240. doi:10.1016/j.jhazmat.2010.05.002
- Chen, D., Zhao, N., Lang, J., Zhou, Y., Wang, X., Li, Y., ... Guo, X. (2018). Contribution of ship emissions to the concentration of PM_{2.5}: A comprehensive study using AIS data and WRF/Chem model in Bohai Rim Region, China. *Science of The Total Environment*, *610*–611, 1476–1486. doi:10.1016/j.scitotenv.2017.07.255
- Comer, B., & Rutherford, D. (2019). Turning the ship, slowly: Progress at IMO on new ship efficiency and black carbon. The International Council on Clean Transportation staff blog. Retrieved from <https://theicct.org/blog/staff/mepc74>
- Fu, Y., Schwebel, D. C., & Hu, G. (2018). Physicians' workloads in China: 1998–2016. *International Journal of Environmental Research and Public Health*, *15*(8), 1649. doi:10.3390/ijerph15081649
- Gong, S. L. (2003). A parameterization of sea-salt aerosol source function for sub- and super-micron particles. *Global Biogeochemical Cycles*, *17*(4), 1097, doi:10.1029/2003GB002079
- Grell, G. A., Peckham, S. E., Schmitz, R., McKeen, S. A., Frost, G., Skamarock, W. C., & Eder, B. (2005). Fully coupled “online” chemistry within the WRF model. *Atmospheric Environment*, *39*(37), 6957–6975. doi:10.1016/j.atmosenv.2005.04.027

- Grell, G., & Baklanov, A. (2011). Integrated modeling for forecasting weather and air quality: A call for fully coupled approaches. *Atmospheric Environment*, 45(38), 6845–6851. doi:10.1016/j.atmosenv.2011.01.017
- Guenther, A. B., Jiang, X., Heald, C. L., Sakulyanontvittaya, T., Duhl, T., Emmons, L. K., & Wang, X. (2012). The model of emissions of gases and aerosols from nature version 2.1 (MEGAN2.1): An extended and updated framework for modeling biogenic emissions. *Geoscientific Model Development*, 5(6), 1471–1492. doi:10.5194/gmd-5-1471-2012
- Hon, G., & Wang, H. (2011). *The energy efficiency design index (EEDI) for new ships*. Retrieved from the International Council on Clean Transportation, <https://www.theicct.org/publications/energy-efficiency-design-index-eedi-new-ships>
- Incentive Partners & Litehauz. (2012). *Economic impact assessment of a NO_x emission control area in the North Sea*. Retrieved from <https://www2.mst.dk/Udgiv/publications/2012/06/978-87-92903-20-4.pdf>
- Janssens-Maenhout, G., Crippa, M., Guizzardi, D., Dentener, F., Muntean, M., Pouliot, G., ... Li, M. (2015). HTAP_v2.2: A mosaic of regional and global emission grid maps for 2008 and 2010 to study hemispheric transport of air pollution. *Atmospheric Chemistry and Physics*, 15(19), 11411–11432. doi:10.5194/acp-15-11411-2015
- Jerrett, M., Burnett, R. T., Pope, C. A., Ito, K., Thurston, G., Krewski, D., ... Thun, M. (2009). Long-term ozone exposure and mortality. *New England Journal of Medicine*, 360(11), 1085–1095. doi:10.1056/NEJMoa0803894
- Kurokawa, J., Ohara, T., Morikawa, T., Hanayama, S., Janssens- Maenhout, G., Fukui, T., Kawashima, K., & Akimoto, H. (2013). Emissions of air pollutants and greenhouse gases over Asian regions during 2000–2008: Regional Emission inventory in ASia (REAS) version 2. *Atmospheric Chemistry and Physics*, 13(21), 11019–11058, doi:10.5194/acp-13-11019-2013
- Lin, H., Liu, T., Xiao, J., Zeng, W., Li, X., Guo, L., ... Ma, W. (2016). Mortality burden of ambient fine particulate air pollution in six Chinese cities: Results from the Pearl River Delta study. *Environment International*, 96, 91–97. doi:10.1016/j.envint.2016.09.007
- Lin, H., Tao, J., Qian, Z. M., Ruan, Z., Xu, Y., Hang, J., ... Ma, W. (2018). Shipping pollution emission associated with increased cardiovascular mortality: A time series study in Guangzhou, China. *Environmental Pollution*, 241, 862–868. doi:10.1016/j.envpol.2018.06.027
- Liu, H., Jin, X., Wu, L., Wang, X., Fu, M., Lv, Z., ... He, K. (2018). The impact of marine shipping and its DECA control on air quality in the Pearl River Delta, China. *Science of The Total Environment*, 625, 1476–1485. doi:10.1016/j.scitotenv.2018.01.033
- Lu, X., Chow, K.-C., Yao, T., Fung, J. C. H., & Lau, A. K. H. (2009). Seasonal variation of the land-sea breeze circulation in the Pearl River Delta region. *Journal of Geophysical Research: Atmospheres*, 114(D17). doi.org/10.1029/2009JD011764
- Lu, X., Yao, T., Fung, J. C. H., & Lin, C. (2016). Estimation of health and economic costs of air pollution over the Pearl River Delta region in China. *Science of the Total Environment*, 566–567, 134–143. doi:10.1016/j.scitotenv.2016.05.060
- Lv, Z., Liu, H., Ying, Q., Fu, M., Meng, Z., Wang, Y., ... He, K. (2018). Impacts of shipping emissions on PM_{2.5} pollution in China. *Atmospheric Chemistry and Physics*, 18(21), 15783–15810. doi:10.5194/acp-2018-540

- Ma, Q., Cai, S., Wang, S., Zhao, B., Martin, R. V., Brauer, M., ... Burnett, R. T. (2017). Impacts of coal burning on ambient PM_{2.5} pollution in China. *Atmospheric Chemistry and Physics*, 17(7), 4477–4491. doi.org/10.5194/acp-17-4477-2017
- Mao, X. (2016). *Action plan for establishing ship emission control zones in China*. Retrieved from the International Council on Clean Transportation, <https://www.theicct.org/publications/action-plan-establishing-ship-emission-control-zones-china>
- Mao, X. (2017). *Marine engine emission standards for China's domestic vessels*. Retrieved from the International Council on Clean Transportation, <https://www.theicct.org/publications/marine-engine-emission-standards-chinas-domestic-vessels>
- Mao, X., Cui, H., Roy, B., Olmer, N., Rutherford, D., & Comer, B. (2017). *Distribution of air pollution from oceangoing vessels in the Greater Pearl River Delta, 2015*. Retrieved from the International Council on Clean Transportation, https://www.theicct.org/sites/default/files/publications/China-GPRD-Baseline-Emissions-Inventory_ICCT-Working%20Paper_23082017_vF.pdf
- Mao, X., & Rutherford, D. (2018a). *Delineating a Chinese emission control area: The potential impact of ship rerouting on emissions*. Retrieved from the International Council on Clean Transportation, <https://www.theicct.org/publications/delineating-chinese-emission-control-area>
- Mao, X., & Rutherford, D. (2018b). *NO_x emissions from merchant vessels in coastal China: 2015 and 2030*. Retrieved from the International Council on Clean Transportation, <https://www.theicct.org/publications/nox-emissions-merchant-vessels-coastal-china-2015-and-2030>
- Mao, X. (2019). *Action plan for establishing China's national emission control area*. Retrieved from the International Council on Clean Transportation, <https://www.theicct.org/publications/action-plan-establishing-chinas-national-emission-control-area>
- National Centers for Environmental Prediction. (n.d.). NCEP FNL operational model global tropospheric analyses, continuing from July 1999. doi:10.5065/D6M043C6
- National Centers for Environmental Information. (n.d.) NECI map application—Hourly/sub-hourly observational data map. Retrieved from <http://gis.ncdc.noaa.gov/maps/ncei/cdo/hourly>
- Olmer, N., Comer, B., Roy, B., Mao, X., & Rutherford, D. (2017). *Greenhouse gas emissions from global shipping, 2013–2015*. Retrieved from the International Council on Clean Transportation, http://theicct.org/sites/default/files/publications/Global-shipping-GHG-emissions-2013-2015_ICCT-Report_17102017_vF.pdf
- Riahi, K., Rao, S., Krey, V., Cho, C., Chirkov, V., Fischer, G. ... Rafaj, P. (2011). RCP 8.5—A scenario of comparatively high greenhouse gas emissions. *Climatic Change*, 109(1-2), 33. doi:10.1007/s10584-011-0149-y
- Rouïl, L., Ratsivalaka, C., André, J., & Allemand, N. (2019). *ECAMED: A technical feasibility study for the implementation of an emission control area (ECA) in the Mediterranean Sea*. Retrieved from The French National Institute for Industrial Environment and Risks, https://www.ineris.fr/sites/ineris.fr/files/contribution/Documents/R_DRC-19-168862-00408A_ECAMED_final_Report_0.pdf
- Rutherford, D., & Miller, J. (2019, March 22). Silent but deadly: The case of shipping emissions. The International Council on Clean Transportation staff blog. Retrieved from <https://www.theicct.org/blog/staff/silent-deadly-case-shipping-emissions>

- Schell, B., Ackermann, I. J., Hass, H., Binkowski, F. S., & Ebel, A. (2001). Modeling the formation of secondary organic aerosol within a comprehensive air quality model system. *Journal of Geophysical Research: Atmospheres*, 106(D22), 28275–28293. doi:10.1029/2001JD000384
- Shanghai International Shipping Institute (2015). *China shipping development outlook 2030*. Shanghai, China: Shanghai International Shipping Institute.
- Shao, Z., & Wagner, D.V. (2015). *Costs and benefits of motor vehicle emission control programs in China*. Retrieved from The International Council on Clean Transportation, <https://theicct.org/publications/costs-and-benefits-motor-vehicle-emission-control-programs-china>
- Shaw, W. J., Allwine, K. J., Fritz, B. G., Rutz, F. C., Rishel, J. P., & Chapman, E. G. (2008). An evaluation of the wind erosion module in DUSTAN, *Atmospheric Environment*, 42(8), 1907–1921. doi:10.1016/j.atmosenv.2007.11.022
- Smith, T. W. P., Jalkanen, J. P., Anderson, B. A., Corbett, J. J., Faber, J., Hanayama, S., ... & Pandey, A. (2015). *Third IMO greenhouse gas study 2014*. Retrieved from the International Maritime Organization, <http://www.imo.org/en/OurWork/Environment/PollutionPrevention/AirPollution/Documents/Third%20Greenhouse%20Gas%20Study/GHG3%20Executive%20Summary%20and%20Report.pdf>
- Sofiev, M., Winebrake, J. J., Johansson, L., Carr, E. W., Prank, M., Soares, J., ... Corbett, J. (2018). Cleaner fuels for ships provide public health benefits with climate tradeoffs. *Nature Communications*, 9(1), 406. doi:10.1038/s41467-017-02774-9
- Stockwell, W. R., Middleton, P., Chang, J. S., & Tang, X. (1990). The second generation regional acid deposition model chemical mechanism for regional air quality modeling. *Journal of Geophysical Research: Atmospheres*, 95(D10), 16343–16367, doi:10.1029/JD095iD10p16343
- Tao, Y., Huang, W., Huang, X., Zhong, L., Lu, S.-E., Li, Y., ... Zhu, T. (2012). Estimated acute effects of ambient ozone and nitrogen dioxide on mortality in the Pearl River Delta of Southern China. *Environmental Health Perspectives*, 120(3), 393–398. doi:10.1289/ehp.1103715
- United Nations Department of Economic and Social Affairs. (n.d.) *World population prospects 2019*. Accessed November 26, 2018, <https://population.un.org/wpp/DataQuery/>
- United Nations, Department of Economic and Social Affairs, Population Division (2017). *World population prospects: The 2017 revision, methodology of the United Nations population estimates and projections (Working Paper No. ESA/P/WP.250)*. New York: United Nations. United Nations Conference on Trade and Development. (2016). *Review of maritime transport 2016*. Retrieved from https://unctad.org/en/PublicationsLibrary/rmt2016_en.pdf
- United Nations Conference on Trade and Development. (2017). *Review of maritime transport 2017*. Retrieved from https://unctad.org/en/PublicationsLibrary/rmt2017_en.pdf
- U.S. Environmental Protection Agency. (2009). *Proposal to designate an emission control area for nitrogen oxides, sulfur oxides and particulate matter* (Technical support document). Retrieved from <https://19january2017snapshot.epa.gov/sites/production/files/2016-09/documents/420r09007.pdf>

- Viana, M., Hammingh, P., Colette, A., Querol, X., Degraeuwe, B., Vlieger, I. de, & van Aardenne, J. (2014). Impact of maritime transport emissions on coastal air quality in Europe. *Atmospheric Environment*, 90, 96–105. doi:10.1016/j.atmosenv.2014.03.046
- Wang, H., & Lutsey, N. (2013). *Long-term potential for increased shipping efficiency through the adoption of industry-leading practices*. Retrieved from the International Council on Clean Transportation, <https://www.theicct.org/publications/long-term-potential-increased-shipping-efficiency>
- Wild, O., Zhu, X., & Prather, M. J. (2000). Fast-J: Accurate simulation of in- and below-cloud photolysis in tropospheric chemical models. *Journal of Atmospheric Chemistry*, 37(3), 245–282. doi:10.1023/A:1006415919030
- Zhang, Y., Yang, X., Brown, R., Yang, L., Morawska, L., Ristovski, Z., ... Huang, C. (2017). Shipping emissions and their impacts on air quality in China. *Science of the Total Environment*, 581, 186–198. doi:10.1016/j.scitotenv.2016.12.098

APPENDIX: COST SENSITIVITY

The SO_x and PM₁₀ compliance costs analyzed in this paper represent the additional cost of burning ECA-compliant fuel. The price assumptions of different fuels, especially the price differentials, significantly impact the cost estimates. Based on assumptions made in Table A1, the cost of fuel-switching and the associated cost-effectiveness corresponding to high-, medium-, and low-price differential scenarios is presented in Table A2.

Table A1. Fuel price estimates for 2030

Fuel type		2015 (2012 \$ per tonne)	2020 (2012 \$ per tonne)	2030 (2012 \$ per tonne)		
				High	Medium	Low
Crude oil		382	454	1212	461	312
MGO		654	554	1481	563	381
LSHFO	High differential	—	—	1185	451	305
	Medium differential			1303	496	335
	Low differential			1422	541	366

Table A2. Fuel price differential scenarios and cost-effectiveness of fuel-switching

Scenario	Additional unit cost of fuel (2012 \$ per tonne)	Total cost of fuel-switching (2012 \$)	Cost-effectiveness of fuel-switching (2012 \$/tonne)	
			PM	SO _x
High differential	112	3.7 billion	27,000	7,300
Medium differential	67	2.2 billion	16,000	4,400
Low differential	22	0.73 billion	5,300	1,400

The cost of NO_x Tier III compliance includes both capital and operational costs of running NO_x aftertreatment. Because real-world applications of these devices on ships are still limited, the cost estimates remain uncertain. Assumptions for the useful life of ships and discount rate also impact the annuity of capital costs, which is the majority of cost of NO_x Tier III compliance. Variations in the cost estimates under scenarios with different combinations of the aforementioned cost variables are summarized in Table A3.

Table A3. CAPEX input scenarios and cost-effectiveness of NO_x Tier III compliance

Scenarios	Useful life (years)	Discount rate	Capital cost	Total cost (2012 \$)	Cost-effectiveness (2012 \$/tonne)
High cost	20	4%	High	247 million	781
Medium cost	25	3.5%	Medium	202 million	638
Low cost	30	3%	Low	153 million	483



www.theicct.org
communications@theicct.org